Karlsruhe Institute of Technology

Master Thesis

Network Flow Models for Power Grids

Franziska Wegner
January 15, 2014

Reviewer: Prof. Dr. Dorothea Wagner and Prof. Dr. Peter Sanders
Advisors: Dr. Martin Nöllenburg
Dr. Ignaz Rutter
Dr. Tamara Mchedlidze

Institute of Theoretical Informatics, Algorithmics
Facility of Informatics
Karlsruhe Institute of Technology

Name:	Franziska Wegner
Student ID:	1612804
Pursued Degree:	Master of Science
Date of Submission:	January 15, 2014
Editing Time:	6 Months

Acknowledgments:

I would like to thank my family and friends for their support; my colleagues for the inspiring discussions, and all reviewers for the helpful suggestions and improvements regarding this thesis.

In addition, I would like to thank TransnetBW for the provided data and, in particular, Guntram Zeitler for the presentation at the TransnetBW substation in Wendlingen and for the discussions and support via mail and in person.

Finally, I would like to thank Prof. Dr. Dorothea Wagner and Prof. Dr. Peter Sanders for the opportunity to work on an exciting interdisciplinary topic.

Contact Information:

Author:
Franziska Wegner
Email: franziska.wegner@student.kit.edu

University:
Karlsruhe Institute of Technology
Kaiserstraße 12
76131 Karlsruhe, Germany
Phone: +49 721 608-0
Fax: +49 721 608-44290
Email: info@kit.edu
`http://www.kit.edu/`

Statement of Authorship:

I hereby declare that this thesis is composed by myself and nobody else, unless otherwise acknowledged in the text or bibliography. Verbatim and contentual borrowed text passages are specifically marked in the document. Furthermore, I follow the constitution of the Karlsruhe Institute of Technology for protection of good academic experience.

Karlsruhe, den 15. January 2014

Abstract

In recent years, power grids and their operation have been becoming increasingly complex due to expanding renewable energy sources, independent power producers and planning of smart energy consumers. Current methods for calculating optimal power flows, which determine the cheapest energy production for each generator and, based on this, determine the electrical flow, rely on non-linear, numerical methods. Here, an electrical flow complies with physical laws and is only seldomly influenced by the network operator. At this point, graph theory, in particular flow algorithms, offer the possibility to efficiently calculate optimal power flows on networks, given the assumption that the flow can be controlled at each node of the network. It is due to the aforementioned compliance with physical laws—and the resulting fact that electrical flows are not controlled—that flow algorithms in electricity networks have been left unattended.

In this thesis, we consider graph-theoretical flow methods in electricity networks and show that these yield electrical flows of considerable quality. We present two approaches: The first approach considers the generator productions of flow models and uses them as input for the power flow method. We use a range of heuristics to obtain physically better generator productions. A second approach tries to implement flows in electricity networks by equipping each node with an electric control system. Arbitrary flow algorithms can then be applied to electricity networks and it turns out that the minimization of production costs and line losses results in a balanced model, which additionally features reduced generator production costs. Moreover, by weighting both criteria, that is, production costs and line losses, the resulting search space is clearly bounded. From an economic point of view, however, introducing control devices at each node of the network is currently not affordable for network providers. For this reason, we combine the flow model for cost minimization and flow balancing with the optimal power flow, such that nodes having control devices and nodes having no such devices can be combined arbitrarily. This model exhibits interesting properties; one of them being the optimal amount of control systems that are necessary to reach the optimal flow. It turns out that only few control nodes are required to gain full control of the electrical flow. For each of the flow models we present experiments using real data to demonstrate the models' properties.

Zusammenfassung

Elektrische Netzwerke und deren Betrieb werden zunehmend komplexer durch die Erweiterung von erneuerbaren Energiequellen, unabhängigen Energieerzeugern und der Planung von intelligenten Energieabnehmern. Aktuelle Verfahren zur optimalen Lastflussberechnung, die die günstigste Energieproduktion für jeden Generator bestimmen und daraus den elektrischen Fluss berechnen, beruhen auf nicht-linearen Methoden aus der Numerik. Dabei folgt ein elektrischer Fluss physikalischen Gesetzmäßigkeiten und wird nur selten von Netzbetreibern aktiv beeinflusst. Die Graphentheorie, im speziellen Flussalgorithmen, bieten die Möglichkeit effizient optimale Flüsse auf Netzwerken zu erzeugen. Es wird jedoch vorausgesetzt, dass an jedem Knoten der Fluss kontrolliert werden kann. Flussalgorithmen wurden daher lange in elektrischen Netzwerken vernachlässigt, da der elektrische Fluss der Physik folgte und nicht gesteuert wird.

Diese Arbeit beschäftigt sich mit graphentheoretischen Flüssen in elektrischen Netzwerken und zeigt, dass Flussmethoden auf elektrischen Netzwerken angewendet werden können, um physikalisch gute Flüsse zu erzeugen. Aus diesem Grunde werden zwei Ansätze vorgestellt: Im ersten Ansatz werden die von den Flussmodellen erzeugten Generatorproduktionen in die Lastflussmethode eingesetzt. Dabei werden eine Reihe von Heuristiken

angewandt, um eine physikalisch bessere Generatorproduktion zu erhalten. Ein zweiter Ansatz versucht Flüsse in elektrischen Netzwerken umzusetzen, indem jeder Knoten mit Steuerelektronik ausgestattet wird. Dadurch können beliebige Flussalgorithmen auf elektrischen Netzwerken angewandt werden und es stellt sich heraus, dass das Minimieren der Produktionskosten und der Leitungsverluste zu einem balancierten Modell führt, welches zudem kostengünstige Generatorproduktionen erlaubt. Durch die Gewichtung der Kriterien Produktionskosten und Leistungsverluste entsteht zudem eine Paretokurve, die den Ergebnisraum klar abgrenzt. Nun wäre aus Netzbetreibersicht ein Steuergerät an jedem Knoten eine unwirtschaftliche bzw. unmöglich zu finanzierende Lösung. Daher wird dieses Flussmodell zur Kostenminimierung und Flussbalancierung mit dem optimalen Leistungsfluss so kombiniert, dass man Steuerknoten und elektrische Knoten ohne Steuerelement beliebig kombinieren kann. Dieses Modell bietet interessante Eigenschaften, die dann auch zur optimalen Anzahl an steuerbaren Knoten im elektrischen Netzwerk führen und zeigen, dass mit wenigen Steuerelementen der Leistungsfluss so beeinflusst werden kann, dass er immernoch zu einer optimalen Lösung führt. Zu allen Flussmodellen werden Experimente anhand realer Daten durchgeführt, um die Eigenschaften der Modelle zu verdeutlichen.

Contents

List of Figures

List of Algorithms

List of Tables

List of Abbreviations

p.u.	Per-Unit System, is a relativ and absolute representation of electrical parameter.
τ	Transformer Tap Ratio
Θ	Phase Angle
B	Shunt Susceptance
C	Condenser
G	Shunt Conductance
P_g	Real Power Generation
Q_d	Reactive Power Demand
Q_g	Reactive Power Generation
R	Resistance
r_s	Series Resistance
R_{pu}	Resistance in per unit
X	Reactance
x_s	Series reactance
X_{pu}	Reactance in per unit
Y	Admittance
Z	Impedance
AC	Alternating Current
DC	Direct Current
DLF	Distribution Loss Factor
FACTS	Flexible Alternating Current Transmission System
IEEE	Institute of Electrical and Electronics Engineers; a world-wide organization for standardization in information technology.

IEP	Improved Evolutionary Program
ILP	Integer Linear Program
IPP	Independent Power Producer
KCL	Kirchoff's Current Law
KVL	Kirchoff's Voltage Law
LMP	Locational Margine Pricing
LP	Linear Program
MILP	Mixed Integer Linear Programs
MVar	Mega Volt-Ampere Reactive, SI derived unit of power; a unit is used in AC electricity networks to distinguish reactive power from real power ($1VAR = 1W = 1V \cdot 1A$).
MW	Megawatt, SI derived unit of power ($1W = 1V \cdot 1A$)
OPF	Optimal Power Flow
OPFSA	Optimal Power Flow Simulated Annealing
PF	Power Flow
PSO	Particle Swarm Optimization
PV	Photo Voltaic
RHS	Right-Hand Side
SA	Simulated Annealing
SCOPF	Security Constrained Optimal Power Flow
SI	International System of Units
SI	Swarm Intelligence
TCUL	Tap Change under Load Transformer
TLF	Transmission Loss Factor
UPFC	Unified Power Flow Controller
V	Voltage

1. Introduction

Power grids, also known as electricity networks, are networks, which satisfy our daily energy demand and consist of generators (producing energy), transmission lines for energy transportation and energy consumers. The energy flows in an electricity network obey laws of physics, and this flow can be hardly controlled. For electrical analysis, like demand satisfaction, costs optimization and fault tolerances, an energy flow calculation is necessary. This results in a non-linear optimization problem that is currently solved by numerical methods known as power flow (PF) to calculate the electrical flow of a given generator production, and optimal power flow (OPF) to calculate the optimal energy production for each generator and the resulting power flow.

Since the complexity and network size w.r.t. power grids has been growing, the efficiency of these flow calculation methods has become increasingly important. Multiple methods based on power flows have been developed recently [45]. However, the direction relating power flow to other types of flows in networks has not been investigated. These flow problems (for example transportation, fluid flows) have the property that the amount of flow on an edge depends only on the capacity of the edge. For this type of problem, traditional flow algorithms well-investigated in theoretical computer science can be applied. To apply flow algorithms on electricity networks, each node has to be able to distribute the flow according to a given flow. Control devices, which are able to influence the electrical flow, are, for example, flexible alternating current transmission systems (FACTS) [44]. In this thesis, we investigate electricity networks under the assumption that either all or a part of nodes are supplied with such a control device. To apply traditional flow algorithms on electricity networks, we initially assume FACTS devices at each node.

We start with investigating power networks where FACTS are placed on each node and as another approach to compare the models with the current OPF method we use the calculated generator productions of the models in the PF method to calculate an electrical flow of the models generator productions. We first apply a simple standard flow model and then remedy its disadvantages. The standard flow model produces an electrical flow, where some transmission lines are close to the thermal limits and a lot of transmission lines are not in use. In order to spread the electrical flow in the network we try to balance the flow on all transmission lines. The first idea to achieve an equally balanced flow is to give all transmission lines the same priority. This is done by minimizing the flow when only half of the transmission line capacity is used. As each transmission line is balanced with the same priority, there are some lines which have more load than others. These transmission lines are called bottleneck lines and contribute potential vulnerabilities in the electricity network. Thus, a second balancing heuristic prioritizes bottleneck edges to balance the flow on these edges and minimizes the maximum edge flow in the electricity network by iteratively reducing the flow on all edges. The standard flow model and both of its balancing variations have high energy production costs, since these models do not take cost functions of each generator into account. Unfortunately, these cost functions are not available in our experimental data. We use the method from Zimmermann et al. [84] to produce generator cost functions from existing data sets. We target to minimize generation costs using the produced cost functions. Additionally, we would like to keep the produced flow balanced. To achieve this we take into account the line losses provided by our data. We claim that the use of line losses results in a decrease of the flow on the bottleneck edges. However, optimizing generation costs and line losses at the same time are two opposing problems. We combine these two optimization functions into one using a weighting optimization method and investigate its solution space.

In the second part of the thesis we make our assumption more realistic and investigate electricity networks, in which only part of the nodes are supplied with FACTS devices. We propose a new model, which merges the electrical power flow model with the graph theoretical flow model with generator and loss minimization. We theoretically investigate the properties of these models and show, e.g., for the 14-bus system [6], that FACTS may provide better solutions in electricity networks. Our case studies with this combined model show for the 14-bus system that only a small number of FACTS is sufficient to provide an optimal solution and to control the whole flow in this electricity network.

Thesis Outline

In Chapter 2, we give an overview of related work on electricity networks and flow algorithms. It presents existing approaches in computer science with regard to electricity networks.

Chapter 3 provides the general notations and definitions of graph theoretical concepts and linear optimization. We introduce different graph types, representations and components, and describe the differences between linear programming and integer linear programming.

Fundamental concepts of electricity networks are presented in Chapter 4. We first describe the standard data format and its components in more detail to understand the structure of such a network. Afterwards, we mention power flow methods, which are part of the optimal power flow calculation, and the approximation of a direct current (DC) electricity network by an alternating current (AC) electricity network.

Chapter 5 provides the results of our investigations of flow algorithms on electricity networks, where FACTS devices are placed on all nodes, or using the calculated generator production of the model in the power flow (PF) method to get the resulting electrical flow. We start with a transformation of an electricity network into a graph-theoretical flow network. To this transformed electricity network we apply several flow models like the standard flow model, two balancing heuristics and a balanced cost minimization model. Each model is established by some case studies.

In Chapter 6, we make the model introduced in Chapter 5 more realistic by assuming that not all nodes can be supplied with FACTS. We prove several theoretical properties of this model. Finally, we describe the results of its case studies.

We summarize this thesis with regards to the results and case studies, and give a brief outlook regarding possible future work in Chapter 7.

2. Related Work

In the first half of the 20th century, power flow calculations and optimal power flow analysis were done by rules of thumb or by tools including slide rules and analog network analyzers. The first publication with regards to digital load flows was provided by Dunstan in 1954 [31], in which he described the *loop and track method*. Since this method includes a complex matrix inversion for which a special data preparation is necessary and since it is strongly limited in network size, an iterative nodal power flow analysis was introduced in 1956 by Ward and Hale [80]. They show that nodal analyses have advantages in contrast to the mesh analysis presented by Dunstan and Henderson [31, 42]. In the same year Shipley and Hochdorf [70] provided different types of load flow solutions as well. In 1957, Brown and Tinney [22] published an iterative nodal method to solve load flow problems automatically. The difference to prior digital solutions is that the digital power analysis from Brown and Tinney has an improved performance, comparable to analog analyzers, and provides the same problem size, while the complexity compared to prior solutions decreases. The first fully optimal power flow formulation was introduced by Capentier in 1962 [24]. Capentier shows that the optimal power flow is a difficult problem for solvers because of its non-linearity. Non-linear solvers cannot guarantee a globally optimal solution, are not robust and are not fast. Therefore, Peschon et al. discuss in their paper from 1968 [63] an efficient computation of the optimal power flow based on the Newton-Raphson method. This method was successfully applied to electricity networks with hundreds of buses. Then, in 1985, a sparsity method for the optimal power flow problem was published by Tinney [75]. In the paper, he emphasizes advantages like data reduction and increasing speed. A survey summarizing past results of optimal power flow in power grids has published in 1991 by Huneault and Galiana [45].

Computer Science Research in Power Grids

There are many research areas in computer science which try to tackle the optimal power flow problem, including fuzzy logic, neural networks, genetic algorithms, artificial intelligence methods, evolutionary computing, ant colony research and particle swarm research. In the following, we present some research in this area.

One of the first works in *fuzzy logic* regarding optimal power flows was presented by Miranda et al. in 1992 [51] using prior results with respect to fuzzy power flow from Miranda and Matos in 1989 [50], and Miranda et al. in 1990 [52]. In this paper, they give a fuzzy model for the optimal power flow problem, where generations and load are modeled as fuzzy numbers. They provide measurements for the robustness and exposure to future scenarios and identify critical network elements. Based on this work, Abdul-Rahman and Shahidepour [14] formulated in 1993 an application for the reactance power planning including static security constraints, while the voltage constraints in each area are modeled as fuzzy sets. A fuzzy multi-objective approach for the optimal power flow problem was published in 1997 by Ramesh and Li [64]. They minimize two conflicting fuzzy goals, which have as objective the secure and economic operation. In 2004, Padhy [61] presented a hybrid model for congestion analysis in an electricity network including both real and reactive power in a deregulated fuzzy environment. As a result, this model provides a congestion-free network by increasing financial benefits. In the same year, El-Saadawi et al. [33] provided a new fuzzy optimization approach to thermal unit commitment (TUC), which involves only thermal units and minimizes the cost of generation, while meeting certain constraints. The demand, reserve requirements and production costs are fuzzy sets used to find an optimal solution by incorporating fuzzy operations and "if-then" rules. A hybrid model for economic dispatching—meaning short-term determination of an optimal generator production—in electrical networks, combining fuzzy adaptive particle swarm optimization and evolutionary algorithms, was published by Niknam in 2010 [54]. In this paper, the hybrid model is accurate and converges quickly; the objective function can be differentiable, non-differentiable, convex or non-convex; and variables can be continuous or discrete. In 2012, Shabani et al. [69] presented a fuzzy-based method for optimal placements of unified power flow controllers (UPFC) to enhance the optimal power flow by using non-linear programming.

Another field in computer science is *evolutionary computing*. The first research work in this areas was presented by Roa-Sepulveda and Pavez-Lazo in 2003 [66]. They present an evolutionary algorithm—simulated annealing (SA)—on electricity networks for an optimal power flow and verify that simulated annealing renders a useful approach to solve the optimal power flow problem. Principally, simulated annealing for optimal power flow (OPFSA) achieves the globally optimal solution, but requires a proper selection of annealing parameters and a long computation time. In 2004, Somasundaram et al. [71] published an evolutionary algorithm for the security constrained optimal power flow (SCOPF) and show that the approach is simple, reliable, efficient and suitable for online applications. Jayabarathi et al. [47] show different evolutionary programming techniques with regards to all kinds of economic dispatch problems in 2005. These evolutionary techniques can find the optimal or nearly optimal solution of all types of economic dispatch problems, including all types of cost functions and a variety of constraints. As for the previous paper, the execution time is long, and therefore not useful in practice. In 2005, from the viewpoint of a generation company, Attaviriyanupap et al. [18] published a paper to optimize the profit of generation companies on deregulated power markets by using evolutionary computing. Ongsakul and Jirapong [58] use evolutionary programming to find an optimal allocation of flexible alternating current transmission systems (FACTS) devices, such that the optimal placement of FACTS improves (maximizes) the total transfer capability (TTC). In 2007, three papers were published regarding optimal power flow, evolutionary computing, and optimal FACTS parameters. The first one, due to Domínguez-Navarro et al. [30], determines optimal FACTS parameters in electricity networks by using evolutionary strategies. It shortly summarizes the possibilities of FACTS in electricity networks and obtains the best point of operation of FACTS devices. The second publication by Sood [72] uses evolutionary programming for optimal power flow (OPF) and validates the results with respect to deregulated power system analyses. The third paper by Ongsakul and Tantimaporn [59] provides an improved evolutionary program (IEP) for optimal power flow, which can be parallized, and therefore reduces the computing time while preserving the quality of the solution. One of the more recent works was published early 2014 by

Reddy and Abhyankar [65] and presents a fast evolutionary algorithm for optimal power flows.

Genetic algorithms (see Goldberg [39]) generally use principles of nature, for example natural selection and survival of the fittest. Genetic algorithms are also used to tackle optimal power flow problems in electricity networks. One of the first publications is due to Walters and Sheble [79], including a reference to the master thesis of Walter [78] in 1991. They present a genetic-based algorithm for the economic dispatch problem. This approach requires several runs to adapt the model, but also shows that genetic algorithms are powerful optimization tools with the advantage of being able to handle any type of unit characteristic data. To provide a solution in large-scale power systems, Chen and Chang [25] present a generic algorithm for economic dispatching for large electricity networks in 1995. In contrast to other genetic approaches, it directly uses a coding, searches for many optimal points in parallel, provides blindness to redundant information and uses probabilistic rules, resulting in a robust and global optimization algorithm. In 2000, Chun and Li [26] showed a hybrid genetic algorithm to solve optimal power flows on electricity networks with FACTS. A genetic algorithm for the optimal allocation and types of FACTS devices in deregulated electricity markets was presented by Cai et al. [23] in 2004. They minimize the system costs function and simultaneously decide the location, types and rating of FACTS devices, which leads to an effective and practical method. Another approach published by Devaraj and Yegnanarayana in 2005 [29] uses generic algorithms for optimal power flows to enhance the security in electricity networks. In this approach, the optimal real power generator production and the phase angles of the phase-shifting transformers are determined. They show that the algorithm is useful in practice, as computation time and space usage is low. In 2006, Todorovski and Rajicic [76] provided an initialization method to overcome the problem of inefficient starting values for voltage angles in genetic algorithms for optimal power flow (OPF). This approach improves the performance of genetic algorithms for optimal power flow.

Swarm intelligence (SI) is a collective behavior observed in nature, where each agent is self-organized. An example for such a behavior are ants. In 2001, Abido [15] published a particle swarm optimization (PSO) for optimal power flows. This new approach provides an efficient and robust method. A more general work from 2008 by del Vallo et al. [28] describes the possibilities of particle swarm optimization in power systems by explaining concepts and variants, since this approach effectively solves large-scale non-linear optimization problems. A survey of particle swarm optimization in electricity networks was given by AlRashidi and El-Hawary in 2009 [16]. With regards to ant colonies, a short-term generation scheduling of thermal power systems was provided by Yu and Song in 2000 [82]. The idea is that co-operating agents like ants work together to find an optimal solution to this problem. This work confirms the applicability of ant colonies to short-term generation scheduling problems of thermal power systems. In 2009, Gasbaoui and Allaoua [36] presented another ant colony optimization approach regarding optimal power flow settings of control variables. They examine the efficiency and robustness of this approach with respect to fuel cost minimization, improved voltage profiles and voltage stability.

This is just a rough overview of some research areas in computer science regarding optimal power flow and FACTS in electricity networks. Unfortunately, these has not yet been any research on graph-theoretical flow algorithms.

Research in Graph-theoretical Flow Networks

The first flow network problem was formulated by Harris in 1954 in the context of rail networks. A possibility to solve the Harris' problem is to use the simplex method provided by Danzig in 1951 [27]. Ford and Fulkerson published the first known flow algorithm and the minimum cut theorem in 1955 [35]. In 1972, Edmonds and Karp [32] improved the time complexity of flow algorithms to $\mathcal{O}(nm^2)$ by providing a shortest augmenting path algorithm. An efficient flow algorithm, named *push–relabel maximum flow algorithm*, was published by Goldberg and Tarjan [37] in 1986 having a runtime of $\mathcal{O}(nm\log(n^2/m))$. The relationship of flow algorithms to the transportation problem is provided by a historical outline by Schrijver in 2000 [67]. In 1990, Goldberg et al. [38] published a detailed survey covering the years 1950 to 1989.

3. Preliminaries

This is a fundamental introduction to the tools that are used in this thesis. The applied terminology for this document is presented below. In addition, a theoretical background concerning computational complexity can be found in Arora and Barak [17], Papadimitriou [62] and Bläser and Manthey [19], and concerning graph theory in Bollobas [21].

3.1. Graph Theory Notation

Directed and Undirected Graph. A *directed graph* is defined by $G = (V, A)$, where the finite sets V and $A \subseteq V \times V$ denote the *vertices* and *arcs*, respectively. The cardinalities of the set of vertices is given by $n = |V|$ and of the set of arcs by $m = |A|$. An arc A is defined by two vertices (u, v), where $u, v \in V$. A vertex u is *incident* to an arc (u, v) if this arc represents an incoming or outgoing arc of vertex u. Two vertices u and v are *adjacent* if they have a common arc $(u, v) \in A$ or $(v, u) \in A$ and the neighborhood is described as $v \in \Gamma(u)$, where v is in the *neighborhood* of u.

For *undirected* graphs we define $G = (V, E)$, where the finite set E represents the edges without a specified direction. That is, each edge $(u, v) \in E$ also includes its reciprocal $(v, u) \in E$. The remaining definitions are similar to those of directed graphs, replacing A by E.

We distinguish between arcs A and edges E to make the difference between directed and undirected graphs obvious.

Capacitive Graph. A *capactive* directed graph is denoted by $G = (V, A, c)$, where $c : A \to \mathbb{R}^m_{\geq 0}$. The function c defines for each arc $a = (u, v) \in A$ a *capacity* $c(a)$. For a capacitive undirected graph $G = (V, E, c)$ the capacity function maps from A to $\mathbb{R}$, i.e., $c : A \to \mathbb{R}$, because each edge allows the flow in both directions. We set $c(u, v) = -c(v, u)$.

Directed Presentation of an Undirected Graph. It is possible to convert an undirected graph into a directed graph without loss of generality. For this each edge $(u, v) \in E$ is represented by two arcs $(u, v), (v, u) \in A$ and a capacity function $c : A \to \mathbb{R}^m_{\geq 0}$, where $c(u, v) = c(v, u)$. Or in other words, the directed representation is formed by the original graph and by its backward graph $\overline{G}$, and therefore $G_{\text{new}} = G \cup \overline{G}$.

Degree. The degree of a vertex u in a directed graph is split into an incoming degree $\mathrm{in}(u)$ of the incoming arcs quantity $|\{(u,v) \in A\}|$ and an outgoing degree $\mathrm{out}(u)$ of the outgoing arcs quantity $|\{(u,v) \in A\}|$. In an undirected graph, $\deg(u)$ denotes the number of edges incident to vertex u.

Cycle. A *cycle* C in a graph $G = (V, E)$ is a set of vertices $C = \{v_i, v_{i+1}, \ldots, v_k\}$, which together build a closed path in G, where $C \subseteq V$. In Figure 3.1, a closed path is $(v_i, v_{i+1}, v_{i+2}, v_i)$. Thus, a cycle is a path, where the starting vertex is also the ending vertex.

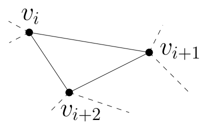

Figure 3.1.: A cycle with vertices v_i, v_{i+1} and v_{i+2}.

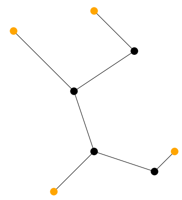

Figure 3.2.: A tree with orange marked leafs.

Tree. A *tree* $T = (V, E)$ is a connected undirected graph without cycles. Thus, there exists exactly one path between each vertex pair in T. The vertex set V is separated into internal vertices with degree greater than 1 and leafs with degree 1. The number of edges in E is $|E| = m = n - 1$. An example is shown in Figure 3.2, where the orange marked vertices are leafs and the black vertices are inner vertices. The number of edges for this example is 7 and the number of vertices is 8, where $m = 8 - 1 = 7$.

3.2. Linear Programming and Integer Linear Programming

Many problems can be formulated as a linear optimization problem, better known as *linear program* (LP) [20, pp.1-26]. Some well-known examples are the minimum-weight or shortest-path problem, the maximum-flow and minimum-cut problem and the transportation problem whose formulations and descriptions can be found in [53, pp. 55-82]. Nemhauser and Wolsey [53, pp. 30-41] present some efficient solvers. In this thesis Gurobi Optimization [5] in combination with MATLAB [7] is used to solve LPs, integer linear programs (ILPs) and their combination.

Linear Programs. Linear programming optimizes an *objective function* z_{LP} subject to certain constraints. Depending on the problem, optimization means that the objective function is minimized or maximized. But it is sufficient to use minimization. In case of maximization the objective function is negated. This also works the other way around.

The problem has to satisfy the following properties to form a linear optimization problem:

- linear objective function $z_{LP} : \mathbb{R}^n \to \mathbb{R}$,
- constraints with linear equations or inequalities.

The objective function consists of a vector $c = (c_1, \ldots, c_n)^T$ representing the constant coefficients (e.g. costs) and a vector of variables $x = (x_1, \ldots, x_n)^T \in \mathbb{R}^n_{\geq 0}$ representing the unknown values which have to be determined. The objective function is defined as

$$z_{\mathrm{LP}} = c^\top \cdot x. \tag{3.1}$$

The constraints consist of a matrix $A \in \mathbb{R}^{m \times n}$, where m is the number of constraints, the above vector x and a restriction vector $b = (b_1, \ldots, b_m)$. The vector b forms the right-hand side (RHS) of the equations. For example:

$$\begin{aligned} a_j \cdot x &\leq b_j, & j &= 1, \ldots, m \\ a_j \cdot x &= b_j, & j &= 1, \ldots, m \\ a_j \cdot x &\geq b_j, & j &= 1, \ldots, m. \end{aligned}$$

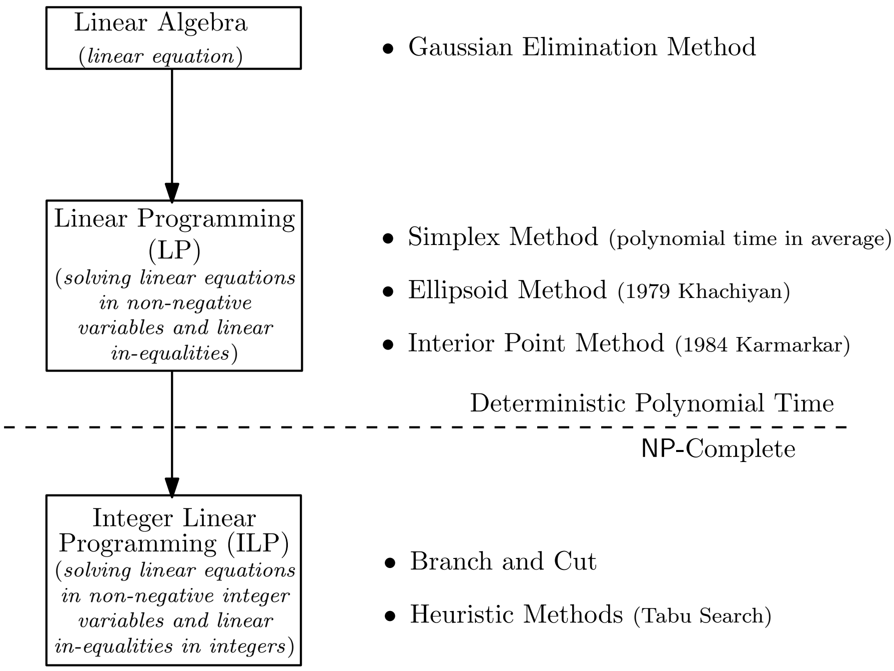

Figure 3.3.: The difference in time complexity of linear programs and integer linear programs is highlighted by the dashed line. Each problem can be solved by the methods listed on the right hand side. The arrows in the figure indicate the increasing difficulty of the methods.

With the non-negativity condition $x_i \geq 0$ the constraints get easier. If x is a free variable, which means it can either be positive, negative or zero, it is possible to convert this free variable into a non-negative variable by setting

$$x_i = x_i^+ - x_i^-,$$

where $x_i^+ \geq 0$ and $x_i^- \geq 0$.

It is possible to transform inequality constraints into equality constraints by simply using slack or surplus variables explained in Examples 1 and 2. Conversely, it is also possible to replace one equality by two in-equality constraints.

Bol [20] shows that linear programs are solvable in deterministic polynomial time. Some methods to solve linear programs are given in Figure 3.3.

Example 1. A *slack variable* is used to transform an inequality into an equality by performing the following step

$$\begin{aligned} & a_j \cdot x && \leq b \\ \Leftrightarrow\ & a_j \cdot x + \text{slack} && = b, && \text{slack} \geq 0. \end{aligned}$$

Example 2. A *surplus variable* is used to transform an in-equality to an equality

$$\begin{aligned} & a_j \cdot x && \geq b \\ \Leftrightarrow\ & a_j \cdot x - \text{surplus} && = b && \text{surplus} \geq 0 \end{aligned}$$

Integer Linear Programs and Mixed Integer Linear Programs. Integer linear programs are used to solve problems, where the variables are integers $x \in \mathbb{Z}^n$. More specifically, it is given by

$$z_{\text{ILP}} = \max\{c^\top x : Ax \leq b, x \in \mathbb{Z}^n_{\geq 0}\},$$

where $b = (b_1, \ldots, b_m)$, $c \in \mathbb{R}^n$ and $A \in \mathbb{R}^{m \times n}$ are given. For ILPs all variables are integer. In a mixed integer linear program (MILP) some variables are restricted to $\mathbb{Z}^{n_i}$ and the other variables are in $\mathbb{R}^{n_j}$. It is denoted by

$$z_{\text{MILP}} = \max\{c^\top x + d^\top y : A_1 x + A_2 y \leq b, x \in \mathbb{R}^{n_x}_{\geq 0}, y \in \mathbb{Z}^{n_y}_{\geq 0}\},$$

where $b = (b_1, \ldots, b_m)$, $c \in \mathbb{R}^{n_x}$, $d \in \mathbb{R}^{n_y}$, $A_1 \in \mathbb{R}^{m \times n_x}$ and $A_2 \in \mathbb{R}^{m \times n_y}$ are given. As shown in Figure 3.3, these problems are NP-complete and a study of their computational complexity is available in Trauth and Woolsey [77].

4. Power Flow in Electricity Networks

Electricity networks, like the one shown in Figure 4.1, satisfy our daily energy demand. Due to the change in the ecological behavior of countries, these networks have been becoming increasingly complex. Thus, the countries have started to employ renewable energy sources, independent power producers (IPP) and smart energy consumers. To analyze the network with regards to demand satisfaction, optimal energy production, fault tolerance and much more, it is necessary to compute a flow of energy in such an electricity network. Energy flows in an electricity network obey elemental laws of physics. To calculate the amount of energy flowing through each edge, traditionally the Power Flow (PF) method is used. In contrast to that, the Optimal Power Flow (OPF) method is used to calculate the electrical flow by minimizing the production costs. Both OPF and PF methods are non-linear optimization problems; they are important tools for network operators and solutions for them have been improving over decades.

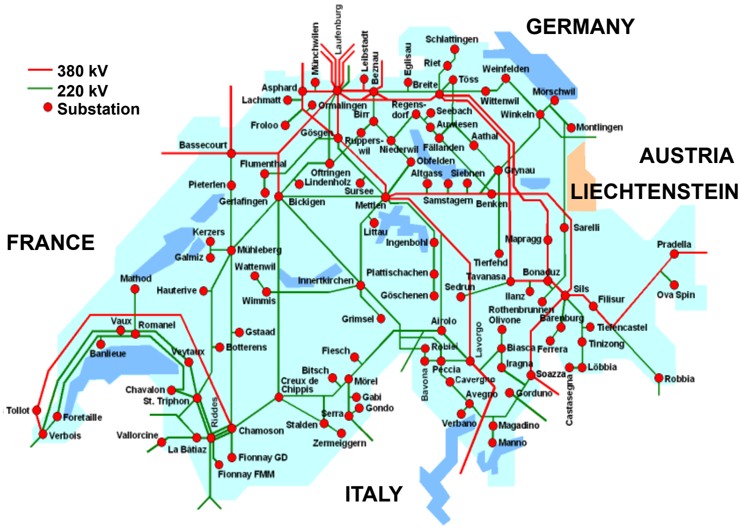

Figure 4.1.: Transmission network of Switzerland from [3].

An electricity network includes multiple components like lines, transformers, generators and much more. In this chapter, we introduce the properties of these components (Section 4.1 and 4.2) and then describe in detail the PF method for both direct and alternating current. We also define a vocabulary which is used throughout this thesis and in the used data from the Washington University [6].

4.1. Transmission Line Parameters

A common way to describe the parameters of an electricity network is provided by the widely-accepted IEEE format described in [40]. A file of this format contains the following fields: *bus data*, *branch data*, loss zones, interchange data and tie lines. In the following, we describe the most common transmission line parameters regarding the example data from the Washington University [6]. Prior to this, however, we describe the structure of an electricity network and the notion of a *per-unit-system*, which is required for the example data set.

General Structure of an Electricity Network. The electricity network shown in Figure 4.2 is called a *14-bus system*, since this electricity network has 14 buses, numbered one to fourteen. It is one of the sample networks from the Washington University [6]. The lines connecting the buses represent the transmission lines and are named *branches*. There can be multiple branches between two buses (see for example the lines connecting buses 1 and 2). An arrow at a bus means that there is a power demand, denoted by S_d, at this bus. S_d consists of real power demand, denoted by P_d, and reactive power demand, denoted by Q_d. Buses with demand are also called *load buses*. Buses which are connected with a *generator* $\mathcal{G}$ (denoted by $\mathcal{G}$) or a *condenser* $\mathcal{C}$ (denoted by $\mathcal{C}$) represent the *generator buses* which are the power supplies in an electricity network. In AC a generator marked with $\mathcal{G}$ has both a *real power output* P_g and a *reactive power output* Q_g, where $\mathcal{C}$ has only *reactive power output* and $\mathcal{G}$ has both real and reactive outputs. The symbols with two separated serrated lines represent *transformers*, which normally change the voltage level.

Per-Unit-System. The power transmitted over a line is denoted by P and is defined as the product of voltage V and current I

$$P = V \times I. \tag{4.1}$$

So, if there is a fixed power that we would like transmit, then we can vary V and I to get this result. As the current I is transmitted over the line, there exist power losses which are determined as

$$P_{loss} = R \times I^2 = R \times \left(\frac{P}{V}\right)^2, \tag{4.2}$$

where R is the resistance, I the current and P_{loss} denotes the line losses. Notice that the resistance R for each line is fixed. Thus, Equation 4.2 shows that, for small current values

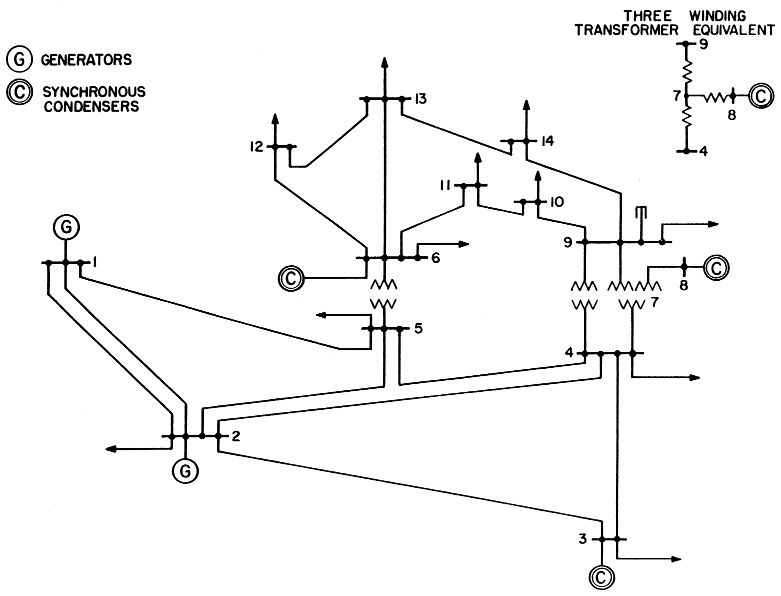

Figure 4.2.: A 14-bus electricity network with five generator buses, eleven load buses and transmission lines.

I, the power losses become vanishingly low. In addition, using high voltages and thereby decreasing the current to reach the transferring power, which is shown in Equation 4.1, results in small line losses, but increases the costs for the transmission system. This results in a trade-off between I and V.

In practice, the high-voltage lines are commonly used in transmission networks for large distance transmissions and low-voltage lines are used in distribution network for short-distance transmissions. Thus, in an electricity network there typically exist multiple *nominal voltage levels*, where nominal voltage denotes the voltage during normal operation. An example of such a network is shown in Figure 4.3, where different voltage levels for different network levels—transmission and distribution—are shown.

To make the calculation in an electricity network with multiple voltage levels easier, the *per-unit-system* is used as a normalization. Within a voltage level each bus voltage is measured with regards to the nominal voltage. The nominal voltage is defined as 1.0 per unit voltage. The following equation represents the conversion into per unit (p.u.):

$$\text{per unit} = \frac{\text{current value}}{\text{base value}} \tag{4.3}$$

Each power grid from the University of Washington [6] described below has a so-called *Mega Volt-Ampere base* (MVA base) for the whole bus system. This MVA base is the power base S_{base}. In transmission systems, as well as in the IEEE examples, it is set

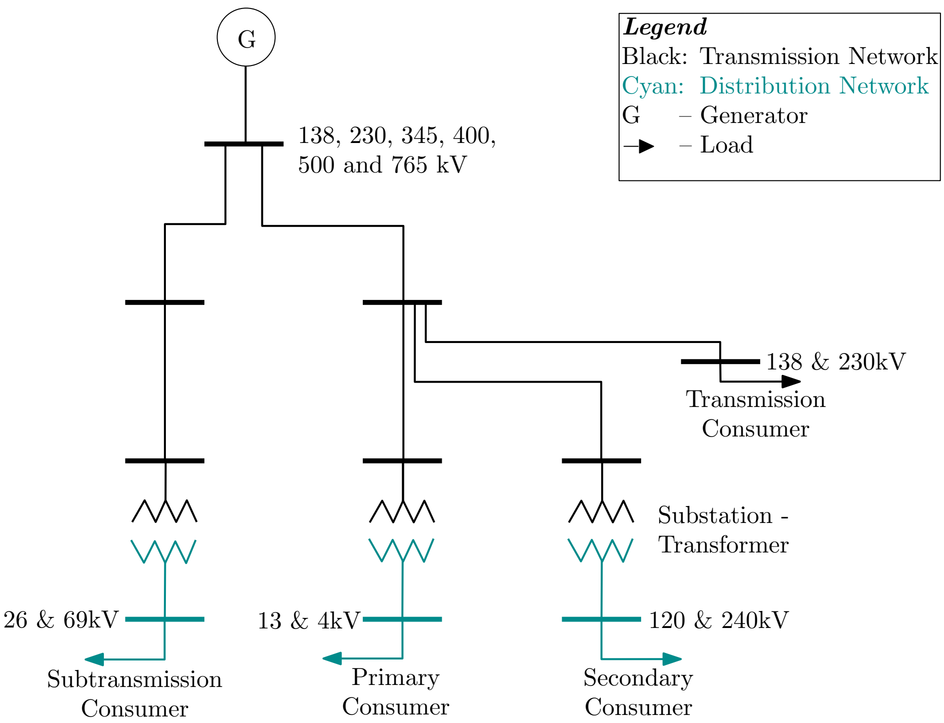

Figure 4.3.: Basic structure of a multi-voltage level electricity network. The network contains a generator $\mathcal{G}$, transmission lines colored in black, step-down transformers and distribution lines colored in cyan. The transformers transform the high voltage to a lower level. Furthermore, there are four different consumers shown with four different voltage levels: a transmission consumer with a high voltage connection and a subtransmission, primary and secondary consumers with medium to low voltage connections. We use the voltage levels and notations described by the U.S.-Canada Power System Outage Task Force [55].

to 100 MVA. Furthermore, the voltage base V_{base} and the current base I_{base} are used to calculate each other.

$$S_{base_{3\phi}} = \sqrt{3} \cdot V_{base_{l2l}} \times I_{base} = 3 \cdot I_{base} \times V_{base_{l2g}}$$

The term $\sqrt{3}\ldots$ is used in the base calculation of a three-phase system only [41]. The same holds for the $V_{base_{l2l}}$, where $l2l$ stands for *line to line* and $l2g$ for *line to ground* [34]. This is the specification of the nominal voltages in a three-phase system. In contrast to power, the current I_{base} is only applied to one of the three phases. These systems are common in AC generation, transmission and distribution networks [74] and are often denoted by 3ϕ. In contrast to this, single-phase systems are denoted by 1ϕ and are common systems for end-user AC power sockets [74].

As shown above, the known electrical formulas can be used for calculating, for example, the impedance Z in per-unit-system:

$$Z_{base} = \frac{V^2_{base_{l2l}}}{S_{base_{3\phi}}} = \frac{V_{base_{l2l}}}{I_{base}}, \qquad Z_{pu} = \frac{Z}{Z_{base}},$$

where Z is in Ω (Ohm). To convert from one base to another, the current per-unit-value is multiplied by the division of Z^{old}_{base} by Z^{new}_{base}:

$$Z^{new}_{pu} = Z^{old}_{pu} \cdot \frac{Z^{old}_{base}}{Z^{new}_{base}} = Z^{old}_{pu} \cdot \frac{\left(V^{old}_{base}\right)^2 \cdot S^{new}_{base}}{\left(V^{new}_{base}\right)^2 \cdot S^{old}_{base}}$$

. **Transformer.** A transformer is a system of coils which turns the voltage at one end (source) into a higher, lower or same voltage at the other end (sink). It is also known as *energy coupling system* and assembled by coils, a core and a casing [43, 73, pp. 131, pp. 103]. The *coils* consist of copper or aluminum windings. These windings are insulated from each other to prevent, for example, shorts. A transformer is made of at least two coils, one at the "from end" (called *primary*) and one at the "to end" (called *secondary*), where the primary coil often denotes the coil at the higher voltage level [43, p. 131]. The *core* is made of magnetic metal like iron. There exist two losses which are influenced by the core: the *hysteresis losses*, which are directly proportional to the volume of the core (or core lamination), and *eddy current losses*, which are directly proportional to the thickness of the core (or core lamination). Large power transformers use many thin laminations of high-grade electrical sheet steel as core [57], which are stacked and insulated to minimize the above losses.

Occasionally, the voltage at the primary end differs from the expected voltage. As the transformer only changes the voltage by a ratio between the primary and secondary coil, the voltage on the secondary coil differs from the expected voltage if the primary voltage differs from the expected voltage. This may result in problems, since the transmission lines and devices in the subnetwork of the secondary coil are made for the nominal voltage. In addition, if the voltage is lower than the nominal voltage, the losses increase. Therefore, on large power transformers, taps are used on the primary coil. These taps work as an offset for any higher or lower voltage input at the primary coil to get the expected nominal voltage at the secondary coil.

The simplified mode of operation is based on a magnetic field within the core, which is created by the primary coil. This generated magnetic flow within the core is denoted by the magnetic flux ϕ. This magnetic flux induces a voltage V_s into the secondary winding. If the number at the secondary coil is less than the one at the primary coil, then the voltage and current decrease, and vice versa.

Bus Data Specification. The bus data describes the available properties of a bus. The sequence of data in the IEEE format [40] is as follows:

1. Bus number

   Each bus has its unique number, which is used for easier handling of the nodes.

2. Name

   Interrelates the bus number with the real name.

3. Load flow area number

   The area number shows in which region or facility the bus is located.

4. Loss zone number

   In addition to the area number, a loss zone number is defined. Zones are normally separated by transformers, and each zone has a different voltage base and therefore different power loss properties (described in Equation 4.2). Zones are used to calculate the transmission loss factor (TLF) and distribution loss factor (DLF) [1]. Therefore, these zones are normally used for locational marginal pricing (LMP) calculation [60].

5. Bus type

   The bus type can be either a *load bus* $l \in \mathcal{L}$ denoted by type 0, *synchronous condenser bus* $c \in \mathcal{C}$ denoted by type 1, *generator bus* $g \in \mathcal{G}$ denoted by type 2 or *reference bus* denoted by type 3. Sometimes there is also an *isolated bus*, which is not mentioned here. There are other bus types details shown in Table 4.1. A load bus of type zero is unregulated and is a demand node only, a bus of type one holds MVar generation within the voltage limits, a generation bus of type two holds reactive and real power generation within limits $Q_{min} < Q_g < Q_{max}$, and type three is given the voltage V and phase angle Θ. The last type is called *swing bus*, *slack bus*, or *v-theta*. In an electricity network, there is always one slack bus necessary to obtain a solution via the numerical power flow methods described in Section 4.3. The last type is often a type-two bus with additional knowledge of voltage V and phase angle Θ.

6. Final voltage

   The final voltage is also known as *voltage magnitude* V. In the power flow modeling, it represents the initial guess for the PF method. This value is denoted by V and expressed in per unit.

7. Final angle

   The final angle, also known as *voltage angle* Θ, is expressed in degrees. In an AC electricity network, voltages and currents oscillate with the same frequency, but are shifted by Θ to each other.

8. Load - real power demand

   Real power demand for one bus is denoted by P_d and measured in mega*watts* (MW).

9. Load - reactive power demand

   Reactive power demand for one bus is denoted by Q_d and measured in mega *volt-ampere reactive* (MVar).

10. Generation - real power output

    Real power produced by a single bus. It is denoted by P_g and measured in MW.

11. Generation - reactive power output

    Reactive power produced by a single bus. It is denoted by Q_g and measured in MVar.

12. Base KV

    In an electricity network, this value is used as a reference quantity of the per-unit-system (p.u.), which simplifies the expression and comparison of parameters in the network.

Table 4.1.: Load flow bus specification from [81].

Bus Type	**P**	**Q**	**|V|**	**Θ**	**Comments**
Load	✓	✓			Usual load representation.
Voltage Controlled	✓		✓		Assume $\|V\|$ is held constant no matter what Q is.
Generator or Synchronous Condenser	✓		✓		Generator or synchronous condenser ($P = 0$) has VAR limits, • Q_{min} minimum Var limit, • Q_{max} maximum Var limit, • $\|V\|$ is held as long as Q_g is within limits.
	✓	✓			
Fixed Z to Ground					Only Z is given.
Reference			✓	✓	”Swing bus” must adjust net power to hold voltage constant (essential for solution).

13. Set point

    A generator bus $g \in \mathcal{G}$ is a voltage controlled bus and its voltage is set by the operators. The reactance power produced Q_g is controlled by changing its reference set point [68, p. 174]. It is specified in per-unit-system.

14. Maximum voltage, MW or MVar limit

    This value is denoted by V_{max} and represents the upper bound for the voltage magnitude of a bus in our case, but it may also describe the maximum real or reactive power. This depends on the user of the IEEE data format.

15. Minimum voltage, MW or MVar limit

    This value is denoted by V_{min} and represents the lower bound for the voltage magnitude of a bus in our case. As above, it may also describe the minimum real or reactive power.

16. Resistors, Capacitors or Reactors - Shunt conductance G

    Is produced by existing electrical fields around resistors, capacitors or reactors and represents an impedance absorption. Therefore, it is represented with a negative sign and its unit is MW. The specification of this parameter in the IEEE sheet is in per-unit-system:

    $$G_{\text{pu}} = \frac{G_{MW}}{S_{Base}}$$

17. Resistors, Capacitors or Reactors - Shunt susceptance B

    Represents an impedance injection measured in MVar. As it is an injection; its sign is positive. Similar to shunt conductance G, the specification of this parameter in the IEEE sheet is in per-unit-system.

$$B_{\text{pu}} = \frac{B_{MVar}}{S_{Base}}$$

Conductance G and susceptance B comprise the real and the imaginary part of admittance $Y = G + j \cdot B$. Both are shown in Figure 4.5.

18. Remote controlled bus number
    Represents the number of the remote controlled bus.

Branch Data Specification. The branch data reconstruct the power grid including restrictions and transmission line parameters. As above, we use the IEEE format [40] to describe the most important line values and properties. A single branch is denoted by (f, t), where f is the from bus and t is the end bus of it.

1. From Bus
2. To Bus
3. Load flow area
   This parameter is already explained in the above bus data specification at Point 3.
4. Loss zone
   Loss zones are described in the above bus data specification at Point 4.
5. Circuit
   Since the electricity network is a multigraph, the number of parallel transmission lines are mentioned with the circuit value. If there is just a single line the value is one.
6. Type
   There are multiple possible line types that can be present:

   0 Transmission line
   Represents a standard branch.

   1 Fixed tap
   For this transformer type, the voltage angle and voltage ratio, which is equivalent to the tap ratio τ, are fixed.

   2 Variable tap for *voltage control* (TCUL, LTC)
   Here, the voltage angle Θ is fixed and the voltage ratio is variable. Load tapchangers (LTC), which keep the voltage at a low level, or tap change under load transformers (TCUL) for voltage control in subtransmission and distribution networks are possible devices.

   3 Variable tap (turns ratio) for *MVar control*
   In this case, the transformer controls the reactive power by a variable voltage ratio. The voltage angle Θ is fixed.

   4 Variable phase angle for *MW control*
   For type four, the voltage ratio is fixed and the phase angle Θ is variable. The real power is controlled by phase shifters, which is described in Point 14.

   The standard transmission line is represented by a type zero. In contrast to this, the other types represent transformer lines. The transformer tap and voltage ratio are

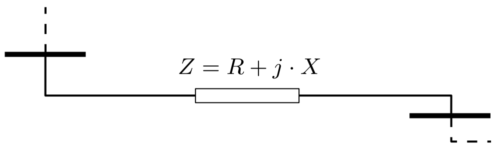

Figure 4.4.: The impedance Z consists of a real term R (resistance) and an imaginary term X (reactance).

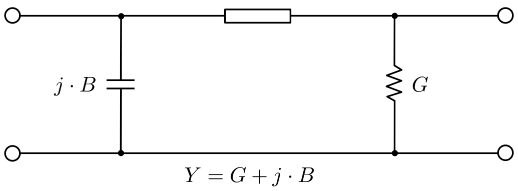

Figure 4.5.: The admittance Y consisting of the conductance G and susceptance B, which represent the real and imaginary part, respectively.

described in more detail at Point 13 and describe the common usage of a transformer, as already described above. The line type which changes the voltage angle by a shift angle Θ_{shift} is described at Point 14 and describes a transformer which, for example, splits the real power P over multiple lines.

7. Resistance

   The branch resistance R_{pu} is expressed in per-unit. Sometimes it is denoted by r or r_s, which denotes the series resistance. It represents the real term of the impedance Z shown in Figure 4.4:

$$R_{pu} = \frac{R}{Z_{base}} \tag{4.4}$$

8. Reactance

   The branch reactance X_{pu} is expressed in per-unit and can also be denoted by a small letter x, or, in case of branches, it is often denoted by x_s, called series reactance. The resistance and reactance define the impedance

$$R_{pu} + j \cdot X_{pu} \tag{4.5}$$

   in per-unit. As shown in Equation 4.5 and in Figure 4.4, it represents the imaginary term.

9. Total Line Charging Susceptance

   This value represents the total line charging susception B in per unit. The description can be found in the above bus data specification at Point 17.

10. Line MVA rating Number 1, 2 and 3

    These values represent the line rating with the lowest value to the left (first value). In our case, the left value represents the normal MVA rating (long term rating), the second value represents the short term value, and the last one represents the emergency value (highest value). The lowest non-zero value is put to the left. These parameters specify the maximum power which can be transmitted over one line. In Germany, there is only one value for a branch, but, for example in France, there exist three values, where the long term capacity is used for the normal operation and the other two capacities represent short term and emergency values, where the branch is shut down after a specified time to prevent branch outages [83]. If the value is zero, then the line is unlimited.

11. Control Bus Number

    The control bus number denotes the bus whose voltage is controlled. If it is controlled by a variable tap transformer for voltage control (branch type 2), then the side at Point 12 has to be specified. Otherwise, if the branch is not of type two, the side is always zero.

12. Side

    The location of the controlled bus is specified by

    0: Controlled bus is one of the terminals,

    1: Controlled bus is on the tap side, and

    2: Controlled bus is on the impedance side (Z bus, see Table 4.1).

13. Transformer tap ratio

    The ratio of turns in the primary coil and those in the secondary coil of a transformer is known as tap ratio and denoted is by τ. For example, if the primary coil consists of nine turns and the secondary coil of three turns, then the turn ratio is 3 : 1. Thus, the voltage at the primary coil is three times greater than at the secondary coil. The turn ratio is equivalent to the voltage ratio and current ratio

    $$\frac{V_p}{V_s} = \frac{I_p}{I_s} = \frac{N_p}{N_s}, \tag{4.6}$$

    where V_p (resp., V_s) is the primary (resp., secondary) voltage, I_p (resp., I_s) is the primary (resp., secondary) current and N_p (resp., N_s) the number of turns of the primary (resp., secondary) coil. The tap is the connection point at the primary windings of the transformer. This tap selects a certain number of windings within the transformer to create the expected voltage at the secondary coil. If the line does not represent a transformer connection, but a standard branch, then the tap ratio is equal to zero.

14. Transformer phase shifter angle

    Transformer phase shifter angles (denoted by Θ_{shift}) are angles which are set in a *phase-shifting transformer* (also known as *phase angle regulating transformer*, *phase angle regulator* or *quadrature booster*). A phase-shifting transformer, in contrast to a standard transformer, controls the real power flow in an AC three-phase electricity network. Particularly, it splits the real power over multiple lines through a phase angle. The purpose of such a power transformer is to handle parallel lines with different voltage level, capacities, or to combine cables and overhead transmission lines. It helps to avoid overloaded cables and therefore stabilizes the network. In addition, these transformers work in both directions.

15. Minimum tap or phase shift

    This entry either describes the minimum tap ratio from Point 13 or the minimum phase shift angle described in Point 14. This depends on the IEEE data format use case.

16. Maximum tap or phase shift

    Similar to Point 15, but using the maximum.

17. Step size

18. Minimum voltage, MVar or MW limit

    Either the minimum voltage V_{min}, reactive power Q_{min} (MVar) or real power P_{min} (MW) limit is described here. This always depends on the use case of the data format.

19. Maximum voltage, MVar or MW limit

    Similar to Point 18, but using the maximum instead.

Generation Costs. As the normal IEEE data does not provide any generation costs, the generator cost functions are built from the existing data set. For this, we use the method described by Zimmerman [84]. If there is a real power generation P_g, the cost function is defined by

$$\gamma = \tfrac{10}{P_g}k^2 + 20k, \tag{4.7}$$

where k is the amount of generation. Otherwise, if there is only a reactive power generation Q_g, the generator costs function is given by

$$\gamma = 0.01k^2 + 40k. \tag{4.8}$$

These functions are necessary to calculate the optimal power flow (OPF), the power flow, that satisfy the demand, minimizes the generation cost [81, 41, 85, 84, 86, 87].

4.2. Properties of Transmission Lines

In the first part, we described the components of an electrical network. In this section, the fundamental properties of an electricity network will be described to prepare for the remaining sections. These properties describe in general, how these components work together. For more details about transmission line properties, we refer to [41, 81]. We start with the two Kirchhoff's laws.

The first Kirchhoff's law, known as *Kirchhoff's current law* (KCL), implies that the incoming current into a bus is the same as the outgoing and it holds for all buses in the electricity network (see Figure 4.6). It is also called *charge conservation law* and is formally written as:

$$\sum_{k=1}^{n} I_k = 0, \tag{4.9}$$

where I is the current and index k is the bus, for $k = 1, \ldots, n$.

The second Kirchhoff's law is the *Kirchhoff's voltage law* (KVL) and describes the behavior of voltages in a loop (also known as mesh) with

$$\sum_{k \in C} V_k = 0, \tag{4.10}$$

where C is the set of buses that comprise a loop and V_k describes the k-th voltage drop (also known as potential drop). Thus, the sum over all potential differences is equal to zero, which is shown in Figure 4.7. This is the *energy conservation law.*

In relation to the two Kirchhoff's laws stands the Ohm's law, which is defined by

$$R = \tfrac{V}{I}, \tag{4.11}$$

where V is the voltage, I is the current and R denotes the resistance. For AC electricity networks, the resistance R is replaced by the impedance Z, which was already mentioned in Section 4.1. It describes the proportionality between current I and voltage V.

4.3. Power Flow

In an electricity network, the flow of the power is mostly determined by both Kirschhoff's laws and Ohm's law. To analyse such networks with regards to, e.g. fault analysis, stability studies and economic calculation, it is necessary to simulate the electrical flow in an electricity network. This is done by power flow analysis methods. There exist two classical power flow analysis methods: the nodal analysis and the loop analysis, which refer to the usage of first and second Kirchhoff's law, respectively.

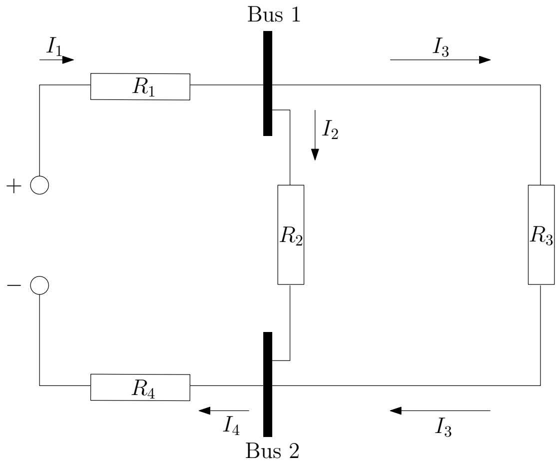

Figure 4.6.: The first Kirchhoff's law, the Kirchhoff's current law, defines that the sum over all incoming and outgoing currents at a bus are equal to zero, for example, $I_1 - I_2 - I_3 = 0$.

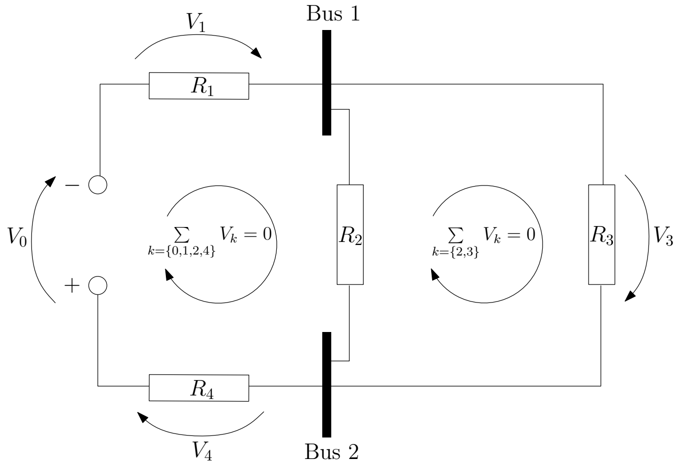

Figure 4.7.: The second Kirchhoff's law, the Kirchhoff's voltage law, defines that the sum over all voltages in a loop are equal to zero, for example, in the second mesh is $V_2 - V_3 = 0$.

The nodal analysis of electrical networks uses the KCL and assigns voltages to the buses of the network with respect to a slack node. The slack node is selected as reference and described in Section 4.1 in the bus specification, Point 5. Thus, if n denotes the number of buses, there exist $n - 1$ equations.

In contrast to the nodal analysis, the loop analysis (also known as mesh analysis) is based on the KVL, where loop currents are calculated for each loop. Here, a reference loop is used instead and there are N equations, where N is the number of loops in the electricity network.

One analysis technique is sufficient to see that both Kirchhoff's laws hold by using Ohm's law for the missing variables. The loop analysis is not a technique for large and complex networks, as it becomes difficult to choose a good reference loop (also known as supermesh) and the loops need to be extracted from the network to apply this analysis. Therefore, the nodal analysis is the preferred to the loop analysis.

For the power flow modeling, the real power demand P_d and reactive power demand Q_d for each bus are given. For each generator bus in the electricity network, the power generation P_g and voltage V are given. And for the slack bus, we know the voltage magnitude V and voltage angle Θ. The goal of such a model is to calculate the voltage magnitudes V and voltage angles Θ at each load bus in the electricity network and voltage angles Θ for the generator buses so that the power demands are satisfied.

Alternating Current Power Flow. In an AC network power consists of two terms: the real power P (measured in MW) and reactive power Q (measured in MVar), i.e., $S = P + jQ$. The data for analysis is given in a steady state as described in Section 4.1. This is sufficient since consumers behavior is predictable. A bus is described by four parameters: voltage magnitude V, voltage angle Θ, real power injection $P = P_g - P_d$ and reactive power injection $Q = Q_g - Q_d$ (see Section 4.1 for more details).

When simulating an electricity network, then it is necessary to include both Kirchhoff's laws. For the nodal analysis, it is sufficient that the KCL holds by satisfying

$$Y \times V - I_g + I_d = 0. \tag{4.12}$$

As the electricity networks are based on power S, including real and reactive terms, it is reformulated to the power base. Power is defined by $S = V \times I$ and therefore we can reformulate the Equation 4.12 by

$$\begin{aligned} & V\left(Y \times V - I_g + I_d\right) = 0 \\ \Leftrightarrow\quad & V\left(Y \times V\right) - S_g + S_d = 0 \end{aligned} \tag{4.13}$$

In total, the electricity network has n buses and Equation 4.13 is represented by $n-1$ equations. These equations include a complex term $Y \times V$. For simplification, these equations are reformulated to real term equations, which results in $2 \cdot (n-1)$ real term equations, consisting of $n-1$ real power equations and $n-1$ reactive power equations:

$$\begin{aligned} P_k &= \underbrace{V_k \sum_{m=\Gamma(k)} \left(V_m \left(g_{km}\cos\left(\Theta_k - \Theta_m\right) + b_{km}\sin\left(\Theta_k - \Theta_m\right)\right)\right)}_{\text{transmission lines transformer, reactors, capacitors, } \cdots} - \underbrace{P_{g_k}}_{\text{production}} + \underbrace{P_{d_k}}_{\text{demand}} \\ Q_k &= \overbrace{V_k \sum_{m=\Gamma(k)} \left(V_m \left(g_{km}\sin\left(\Theta_k - \Theta_m\right) + b_{km}\cos\left(\Theta_k - \Theta_m\right)\right)\right)} - \overbrace{Q_{g_k}} + \overbrace{Q_{d_k}} \end{aligned} \tag{4.14}$$

Equations 4.14 are for all buses m incident to bus k, where index k denotes the observed bus, for $k = 1, \ldots, n$. The components g_{km} and b_{km} are part of the admittance, which is described in Section 4.1 at Point 17. Equations 4.14 are non-linear equations, since they include $sin(x)$ and $cos(x)$. In Section 3.2, we described methods to solve linear equations, but not non-linear ones. In this case, an iterative numerical method is necessary. One of the most popular methods is the Newton-Raphson method. The approach starts with an estimation of the unknown variable x_0 with voltage V_0 and voltage angle Θ_0 (also known as initial guess) and then $f(x)$ is written as Taylor series:

$$f(x) = f(x_0) + \left(\left.\frac{\partial f}{\partial x}\right|_{x=x_0}\right)(x - x_0) + \frac{1}{2}\left(\left.\frac{\partial^2 f}{\partial x^2}\right|_{x=x_0}\right)(x - x_0) + \cdots \tag{4.15}$$

For the Newton-Raphson method the Taylor series can be cut after the second term, since the remaining part is negligible. This results in a linearized equation system. For the power flow equation it holds that the sum is equal to zero. Therefore, $f(x) = 0$ and

$$x_i \approx x_0 - \left(\left.\frac{\partial f}{\partial x}\right|_{x=x_0}\right)^{-1} f(x_0). \tag{4.16}$$

The Newton-Raphson method is an iterative method, where in each iteration the error Δx decreases and the convergence depends on the initial guess x_0, but converges fast. As we talk about AC power equation, the non-linearity leads to possibly multiple results, where the initial guess also determines to which solution the method converges.

Revert to the nodal analysis the Equation 4.15 forms a matrix, where f represents the real and reactive power in Equation 4.14, and x the voltage magnitude V and voltage angles Θ. The Jacobian matrix is

$$J(\Theta, V) = \begin{pmatrix} \frac{\partial P_1}{\partial \Theta_1} & \frac{\partial P_1}{\partial V_1} & \frac{\partial P_1}{\partial \Theta_2} & \frac{\partial P_1}{\partial V_2} & \cdots & \frac{\partial P_1}{\partial \Theta_{n-1}} & \frac{\partial P_1}{\partial V_{n-1}} \\ \frac{\partial Q_1}{\partial \Theta_1} & \frac{\partial Q_1}{\partial V_1} & \frac{\partial Q_1}{\partial \Theta_2} & \frac{\partial Q_1}{\partial V_2} & \cdots & \frac{\partial Q_1}{\partial \Theta_{n-1}} & \frac{\partial Q_1}{\partial V_{n-1}} \\ \frac{\partial P_2}{\partial \Theta_1} & \frac{\partial P_2}{\partial V_1} & & & & \frac{\partial P_2}{\partial \Theta_{n-1}} & \frac{\partial P_2}{\partial V_{n-1}} \\ \frac{\partial Q_2}{\partial \Theta_1} & \frac{\partial Q_2}{\partial V_1} & & & & \frac{\partial Q_2}{\partial \Theta_{n-1}} & \frac{\partial Q_2}{\partial V_{n-1}} \\ \vdots & & & & \ddots & & \vdots \\ \frac{\partial P_{n-1}}{\partial \Theta_1} & \frac{\partial P_{n-1}}{\partial V_1} & & & & \frac{\partial P_{n-1}}{\partial \Theta_{n-1}} & \frac{\partial P_{n-1}}{\partial V_{n-1}} \\ \frac{\partial Q_{n-1}}{\partial \Theta_1} & \frac{\partial Q_{n-1}}{\partial V_1} & & & \cdots & \frac{\partial Q_{n-1}}{\partial \Theta_{n-1}} & \frac{\partial Q_{n-1}}{\partial V_{n-1}} \end{pmatrix} \tag{4.17}$$

The linearized equation system is solved for the next iterations by using the next estimation for voltage magnitude V and voltage angle Θ. This iteration ends if the error Δx lies in the tolerance ϵ. Typical initial guesses are $V_0 = 1$ for voltage magnitude and $\Theta = 0$ for voltage angles or there may exists past results. This provides just a short overview of the power flow problem. Further information are available at [81, 41].

4.4. Direct Current Approximation

Often it is sufficient to assume that the considered network is a DC network. This simplification provides a linear model and considers only the real part $p_f = \mathcal{R}(s_f)$ of the AC power network. As the DC electricity network is linear, the methods mentioned in Section 3.2 can be applied to calculate the voltage magnitudes V and voltage angles Θ. Examples for using a DC approximation instead of an exact AC model are shown in [60].

To approximate an AC network with a DC one four simplification are applied from [81, 85, 84, 86, 87].

1. As the real part of the power S is used, while the reactive power Q is neglected.
2. The branches in a DC electricity network are assumed to be lossless lines. From Section 4.1 follows, that the series resistance r_s and charging capacitance b_c are negligible. Thus, the series admittance y_s for $r_s \approx 0$ and $b_c \approx 0$ can be written as

   $$y_s = \frac{1}{z_s} = \frac{1}{r_s + jx_s} \approx \frac{1}{jx_s}. \tag{4.18}$$

   As the branches are assumed to be lossless, the power injection at both ends of the branch is the same, but negative, since the power flows into the other direction, that is,

   $$p_f = -p_t. \tag{4.19}$$

3. The bus voltage magnitudes are close to one per unit, such that

   $$v_i \approx e^{j\Theta_i}. \tag{4.20}$$

4. Voltage angle difference $\Delta\Theta$ is very small over all branches, i.e., it can be assumed that:

   $$\sin(\Theta_f - \Theta_t - \Theta_{\text{shift}}) = \Theta_f - \Theta_t - \Theta_{\text{shift}} \tag{4.21}$$

By using these assumptions, Zimmerman et al.[85] show that the relationship between real power flow and voltage angles for a branch i is given by

$$(p_i) = B_i(\Theta_i) + (P_{\text{shift}_i}), \tag{4.22}$$

where (p_i) is a vector with entries for each bus, B_i is the adjacency matrix multiplied with $b_i = 1/(x_{s_i}\tau_i)$, and (P_{shift_i}) is a vector with entries for each bus, where $P_{\text{shift}_i} = b_i \cdot \Theta_{\text{shift}}$. The B matrix can be seen analogously to the admittance matrix of the AC electricity network. Thus, the DC power balancing equation of the nodal analysis is given by

$$g_p(\Theta, P_g) = B \cdot \Theta + P_{\text{shift}} + P_d + G_{sh} - P_g = 0. \tag{4.23}$$

Function g_p in Equation 4.23 is also called mismatch.

5. Flow-Based Approaches

This chapter addresses the topic graph theoretical flows in electricity networks. The goal is it to show that it is possible to apply graph theoretical flows on electricity networks thereby obtain good physical flows. Applying flows on electricity networks implies slight changes to the network. Each vertex has to include electric control systems, for example flexible alternating current transmission systems (FACTS). After having explained the transformation of an electricity network, these transformed networks are used by our models. We start with a standard flow model and improve this model with regards to existing problems, such that we get two balancing heuristics, where the first balances the flow uniformly and the second one prioritize bottleneck edges. The standard flow and its variants have too high generator production costs. Therefore, we optimize the flow with regards to generator productions, but balancing has to be achieved, too. That is, the model includes the minimization of the line losses, to become balanced. Within the case studies, we apply these flows directly on the network and get a solution for a network with FACTS at each node. But to use these models in a realistic context, which means that there are only a few FACTS in the electricity network, the generator production of these models is inserted in a power flow (PF) calculation. This approach uses the standard method to calculate electrical flows and shows the behavior of an electrical flow by using different generator productions of different models.

The fundamentals for flow algorithms and linear programming were introduced in Chapter 3. In addition, all models are implemented in MATLAB R2013a by using Gurobi 5.5.0.

5.1. Transformation to an s-t-Graph

To apply flow models on electricity networks or other networks it is necessary to transform these networks to s-t-networks with one source and one sink to generate flows. Therefore, we interpret the electricity networks with regard to graph theoretical terms and define the sources and sinks of these network structures to connect these sources (resp., sinks) to one supersource s (resp., supersink t). This transformation also simplifies the work in the graph theoretical area and provides clear mathematical descriptions.

Given an electrical network $N_E = (\mathcal{B}, \mathcal{G}, \mathcal{L}, \mathcal{T}, \mathcal{C}, \mathcal{D}, c_E, \gamma_E, \ell_E, B_E, P_{\text{shift}_E}, \dots)$ as shown in Figure 4.2 with a set of buses $\mathcal{B}$ and a multiset of transmission lines $\mathcal{D}$, each connecting

Table 5.1.: Merging parallel transmission lines results in an adaption of the electrical parameters. An edge $e_j \in E_j$, where E_j is a set of duplicates with $E_j \subseteq E'$ and E' is a multiset. The quantity of duplicates is denoted with $k_j := |E_j|$. All edges e_j incident to u and v with $k_j > 1$, are merged to one single edge $e_j : (u, v) \in E$, where E is a single set, for each $j = 1, \dots, k_j$. By replacing $\square$ with the parameter identifier, the total parameter is calculated for these transmission lines, e.g., for resistance: $\square$ is replaced by R.

	$\square = \sum_{i=1}^{k} \square_i$	$\square = 1/\sum_{i=1}^{k} \frac{1}{\square_i}$	$\square = \square_1 = \square_2 = \dots = \square_k$
Real Power P	✗		
Reactive Power Q	✗		
Capacity c	✗		
Current I	✗		
Admittance Y	✗		
Resistance R		✗	
Inductivity L		✗	
Impedance Z		✗	
Voltage U			✗

two buses. A bus can be a transformer $t \in \mathcal{T}$, or can be connected with a generator $g \in \mathcal{G}$, a consumer $l \in \mathcal{L}$, a transformer $t \in \mathcal{T}$, a condenser $k \in \mathcal{C}$ and other electrical components, where $\mathcal{B} = \mathcal{G} \cup \mathcal{L} \cup \mathcal{T} \cup \mathcal{C}$. These components were described in more detail in Chapter 4. Furthermore, network N_E provides functions like c_E, γ_E, ℓ_E, B_E, P_{shift_E} and others, where

- $c_E : \mathcal{D} \to \mathbb{R}$ is the capacity on the transmission lines;
- $\gamma_E : \mathcal{G} \to \mathbb{R}_{\geq 0}$ is the generation cost (or production cost) of a generator $g \in \mathcal{G}$;
- $\ell_E : \mathcal{D} \to \mathbb{R}_{\geq 0}$ describes the losses of all transmission lines in $\mathcal{D}$ dependent on resistance R of each line;
- $B_E : \mathcal{D} \to \mathbb{R}_{\geq 0}$ is dependent on reactance X and tap ratio τ and is defined in interval $(0, 1]$;
- $P_{\text{shift}_E} : \mathcal{D} \to \mathbb{R}_{\geq 0}$ describes the transformer shift angles, where phase angles regulating how the transformer distributes the power over multiple lines between two buses by changing the transformer shift angles;
- electrical networks provide much more data and include much more devices as suggested in Chapter 4, which are not of interest for this thesis.

To transform $N_E = (\mathcal{B}, \mathcal{G}, \mathcal{L}, \mathcal{T}, \mathcal{C}, \mathcal{D}, c_E, \gamma_E, \ell_E, B_b, P_{\text{shift}}, \dots)$ to a capacitive s-t-network $N_{st} = (G = (V, E), c, \gamma, \ell, B_b, P_{\text{shift}})$ we define that each bus $b \in \mathcal{B}$ is represented by a vertex $u \in V$, where $|V| = n$ (shown in Figure 5.1a). Transmission lines between two buses u and v corresponds to edges $(u, v) \in E'$, where E' is a multiset. The multigraph G' is then transformed to a simple graph G (in N_{st}), which is shown in Figure 5.1b. By merging parallel lines, the following parameters must be adapted: real power P, reactive power Q, resistance R, reactance X, capacity c, voltage U, current I, inductivity L, impedance Z, admittance Y and all related parameters, which is shown in Table 5.1.

Buses connected to generators in $\mathcal{G}$, which are responsible for real and reactive power, and condensers in $\mathcal{C}$, which are responsible for reactive power, are connected to an additional vertex s (see Figure 5.1c), which is called *source*. Buses connected to consumers in $\mathcal{L}$ (also known as buses with load) are connected to an additional vertex $t \in V$, called *sink* also shown in Figure 5.1d. Transformers in $\mathcal{T}$ and other components need no special modeling,

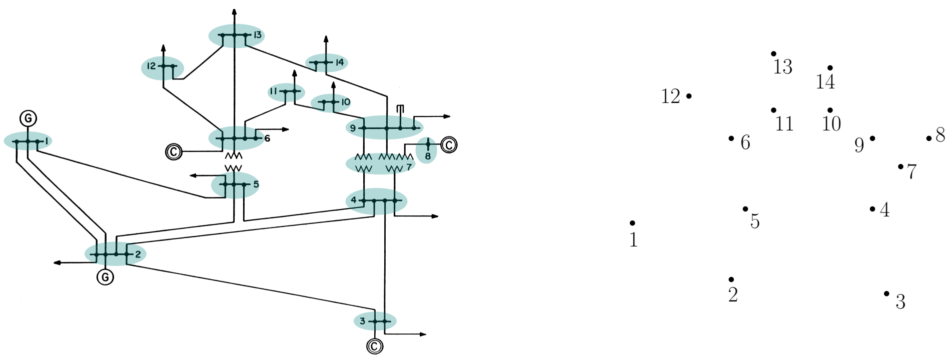

(a) The highlighted areas on the left side are buses $b \in \mathcal{B}$ in N_E. These buses are represented by vertices $v \in V$ in N_{st} shown on the right side.

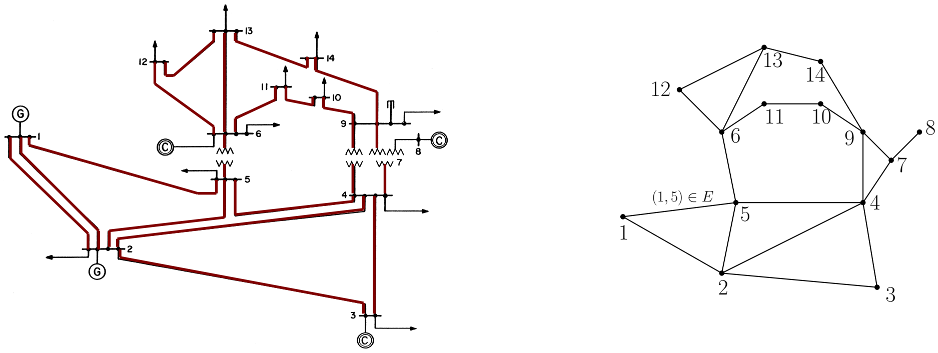

(b) A Network N_E can have multiple transmission lines per bus pair (highlighted red). These transmission lines are represented by edges $(u, v) \in_k E'$ and the resulting multigraph G' is modified to a simple graph G in N_{st}, such, that there is only one edge per vertex pair.

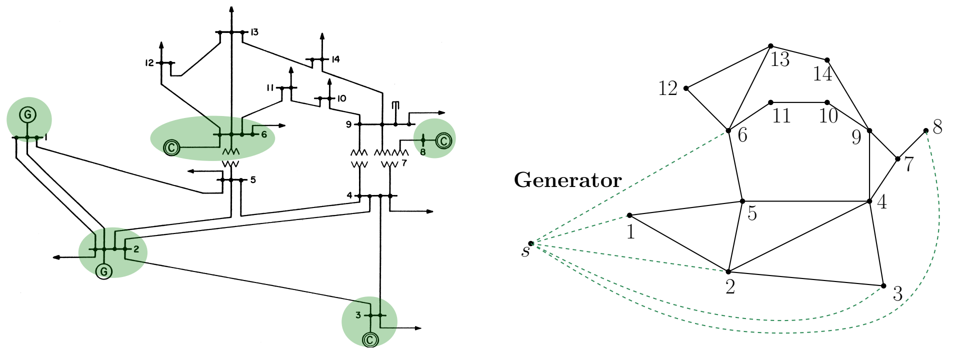

(c) Buses $b \in \mathcal{B}$ which are connected with a real and/or a reactive power generator (highlighted green) are connected with a vertex s, known as source.

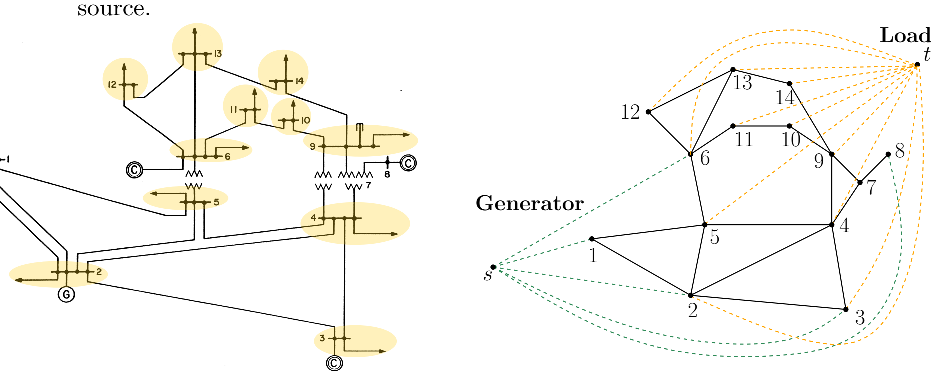

(d) Loads in N_E are represented by an arrow (highlighted yellow) and buses $b \in \mathcal{B}$ connected with a load are expressed with an edge to a vertex t, known as sink.

Figure 5.1.: Transformation of an electricity network N_E (left side) to a s-t-network N_{st} (right side) using a 14 bus system [6] as example.

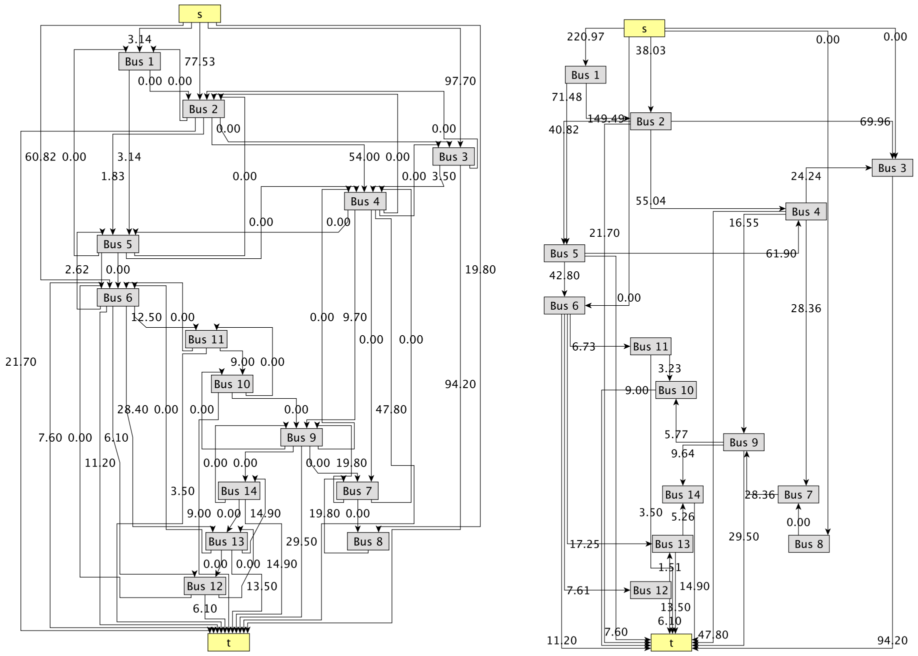

(a) Flow f_{std} of the standard flow model in the electrical network N.

(b) Flow f_{opf} of the optimal power flow model in the electrical network N.

Figure 5.2.: The electricity network N is the 14-bus network from the Washington University [6]. The helper vertices s (source) and t (sink) are highlighted in yellow.

as they are parameters in the data set, which are used in functions. Function c, γ, ℓ, B and P_{shift} are defined for N_{st} the following way:

- $c : E \to \mathbb{R}_{\geq 0}$ is the edge capacity;
- $\gamma : E \to \mathbb{R}_{\geq 0}$ is the generation cost where $\gamma(u, v) = 0$ if $s \notin \{u, v\}$;
- $\ell : E \to \mathbb{R}_{\geq 0}$ describes the losses, which are defined to be zero for all edges adjacent to s and t;
- $B : E \to \mathbb{R}_{\geq 0}$ is the inverse reactance defined in interval $(0, 1]$ and
- $P_{\text{shift}} : E \to \mathbb{R}_{\geq 0}$ describes the transformer shift angles and is mostly zero.

The source vertex s has the total amount of power production of all generators in $\mathcal{G}$ and condensers in $\mathcal{C}$. The edge capacity for edges $(s, u) \in E$ for all $u \in V$ corresponds to the maximum production for the generator $g \in \mathcal{G}$ and condensers $k \in \mathcal{C}$ at u. The sink vertex t owns the total amount of load of all consumers $l \in \mathcal{L}$. Edge capacities for $(v, t) \in E$ for all $v \in V$ are equivalent to the load at vertex v.

5.2. Standard Flow Model

Electrical flows, which we call power flows, are physically predetermined. Since the electrical flow uses laws of physics, there is just a little control in current electricity networks provided by a few flexible alternating current transmission system (FACTS). Modeling a standard flow on an electricity network expects at each vertex, that there exists a full control over the power flow. Therefore, we assume FACTS at all vertices, which provides us the necessary control, and the transformation of the electricity network described in the previous section is used to apply flows. Our intention is to see problems or a behavior while applying this standard flow model to electricity networks, which gives us an idea of possible improvements. Within the case study, we use the flow directly produced by the standard flow on an electricity network to understand the flow behavior and in addition to that, we use the generator productions of the standard flow model in the PF method to achieve realistic flows on electricity networks. This section describes the mathematical model of a standard flow and the corresponding experiments.

We realize a minimum cost flow, where we apply the same cost to each edge. The flow has to satisfy the flow conservation for each vertex, which means that the outgoing flow at a vertex is the same as the incoming flow. This can be related to the Kirchhoff's current law (KCL) described in Section 4.2. Furthermore, the flow on each edge is limited with regards to the capacity function in an electricity network, which is related to the thermal limit of a transmission line. The objective function represents the flow costs, which we minimize.

Mathematical model description. An electricity network $N = (G = (V, A), c, s, t)$ is a capacitive graph G with vertex set V and arc set A. In addition, this network includes a source s and a sink t, and a function $c : A \to \mathbb{R}$, which describes the arc capacities. Since we use a direct representation of an undirected graph (see Section 3.1), $c(u, v) = c(v, u)$ for all $(u, v) \in A$.

Let N be an electricity network and let $f : A \to \mathbb{R}$ be a function. Function f is called a *feasible flow* on N, if it satisfies the flow conservation

$$\begin{aligned} \sum_{v \in V} f(u,v) &= 0 && \forall\, u \in V \setminus \{s,t\} \\ \sum_{u:(s,u)\in A} f(s,u) &= \sum_{v:(v,t)\in A} f(v,t) = \sum_{v:(v,t)\in A} c(v,t) && \forall\, \{u,v\} \in V \setminus \{s,t\} \end{aligned} \tag{5.1}$$

and in addition, the capacity constraints

$$f(u,v) \leq c(u,v) \qquad \forall\, (u,v) \in A. \tag{5.2}$$

The *network cost* for network N and function f is the following:

$$z(N,f) = \sum_{(u,v)\in A} f(u,v) \tag{5.3}$$

The flow $f(u, v)$ is understood as a variant and the Equations 5.1 and 5.2 denote the linear constraints. By minimizing the objective function in Equation 5.3 subject to these linear constraints, a linear program is formed, which we denote as *standard flow LP*. It minimizes the costs of a flow.

Case Study. In the case studies we use two approaches to compare the models. The first on is to assume FACTS at each vertex in the electricity network. This approach allows us to apply the model on the electricity network and the flow can be directly compared with the one of the OPF. Since the resulting flow is—in most cases—totally different to the one of the OPF, as it does not model any physical laws, and it is not easy to declare if the flow is good or not, we provide a second approach to compare the models. In this approach, we insert the generator production of the model (here the standard model) and insert it in the PF method. This shows us the electrical flow of the calculated generator production and the model results can be used in a realistic electricity network without FACTS (or just a few FACTS).

Applying a standard flow model on an electrical network N generates a flow f_{std} on N, which is shown for the bus network 14 from the Washington University [6] in Figure 5.2a.

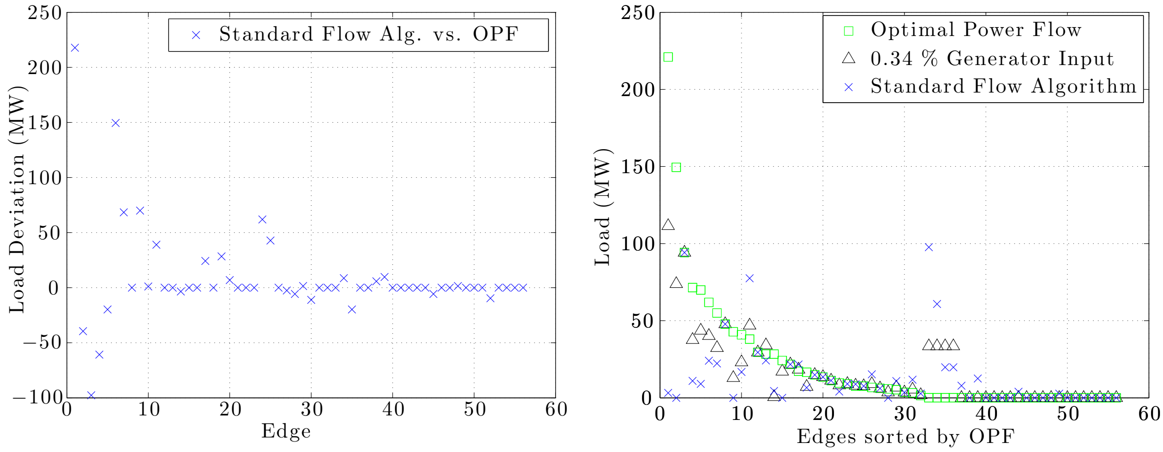

(a) Edge flow deviation between the optimal power flow model (OPF) and a standard flow model in N is plotted with $f_{\text{opf}}(e_i) - f_{\text{opf}}(e_i)$ for all $i = 1, \ldots, n$. The edges are sorted by the original graph input.

(b) The standard flow generator production and a dummy production are included in the power flow(PF) calculation. For comparison the optimal power flow(OPF) is plotted and all edges are sorted decreasing with regards to the OPF.

Figure 5.3.: Plots for the 14 bus electrical network N from the Washington University [6] using the standard flow model.

The network N in Figure 5.2a represents a directed representation of an undirected network (see Section 3.1). For the optimal power flow f_{opf} in Figure 5.2b the network N is an undirected graph.

To compare the flow f_{std} in N of the standard flow model and the OPF f_{opf} in N, we take a closer look at the edge flow deviation in Figure 5.3a. Figure 5.3a shows, that the biggest deviations are located in the first ten edges, where the edges are in the original data set order. More specific, the main difference is in the power generation on edges $(s, u) \in E$ for all $u \in V \setminus \{s, t\}$, e.g., the edge $e_1 = (s, \text{Bus1})$ has a deviation of 217.82 MW. Of course, as there exist five generators, the missing power production is distributed to the other four generators. The reason for this behavior is that we do not take into account any generator parameters, apart from the capacities.

Another conspicuity is that some edges are included in the flow f_{std} of the standard flow model, but not in the OPF flow f_{opf} and vice versa. Furthermore, a possible problem can be high loaded edges close to the capacity, also known as bottleneck edges.

Summarizing, this simple model gives us information about possible problems:

- Arcs may overloaded in a network with worse generator distribution,
- No balancing of generation and flow, and
- Production costs are disregarded.

The last point becomes clear, if we compare the production costs of the OPF with 7642 USD, and the standard flow model with 10386 USD. Thus, the production costs has to be included in the model to get an economical suggestive result.

In addition, if we use the generator production of the standard flow model in the power flow model (see Figure 5.3b), the electrical flow calculated by the power flow model results in a totally different flow. In Figure 5.3b, the peaks at edge e_{11}, which corresponds to edge $(s, \text{Bus2})$, and edge e_{33} corresponding to edge $(s, \text{Bus3})$ show that the main flow differences are at the generators, but it also shows that in a network with a good generator distribution the maximum flow on an edge is low, because the production is located close to the consumption.

5.3. Balanced Flow Model

The experimental evaluation of the standard flow model from Section 5.2 shows that there are some problems. One of them is an unbalanced flow, where the edge flows are close to the capacity, which may produce bottlenecks and leads to faster attrition. Capacities of transmission lines are thermal limits, and therefore a convergence to this limit stress these lines. For that, the flow has to be balanced to relieve these edges and to provide a more robust flow. The idea is to balance all edges uniformly by minimizing the difference to half of their capacity. We show how to model a flow on an edge pair (u, v) and (v, u), while using just one edge of them. In addition, we combine the balancing ideas with the previous model, which includes the conservation of flow on each vertex, the capacity constraints on each edge and the cost minimization. This section introduces the mathematical model for a uniform balancing and provides examples to see further problems and improvement capabilities. As for the previous model, two evaluation variants are used to interpret this model with regards to electricity networks. The first variant applies the flow directly to the network and the second one uses the calculated generator productions in the PF method.

Mathematical model description. The electrical network $N = (G = (V, A), c, s, t)$ is the same network as defined in the previous section. In addition, f is a *flow* in N if it satisfies the flow conservation and capacity constraints from Equations 5.1 and 5.2.

Let N be an electrical network, let $y(u, v) \in \{0, 1\}$ with $y(u, v) = y(v, u)$ for all $(u, v) \in A$. A *feasible function* f in N is given by

$$\begin{aligned} f(u,v) - \ & y(u,v) \cdot c(u,v) \ \leq 0, \\ f(v,u) + \ & y(v,u) \cdot c(v,u) \ \leq c(v,u). \end{aligned} \tag{5.4}$$

Equation 5.4 conveys, that the flow is restricted to one of the edges per vertex pair (u, v) and (v, u).

Let N be an electricity network. We would like the flow on each edge $(u, v) \in E$ to be as close to 50% of the maximum load as possible, that is

$$f(u,v) + f(v,u) \approx \tfrac{c(u,v)}{2}. \tag{5.5}$$

By subtracting $c(u, v)/2$ from this approximation we ideally obtain a term close to zero, that is

$$f(u,v) + f(v,u) - \tfrac{c(u,v)}{2} \approx 0. \tag{5.6}$$

We introduce a term $\Delta(u, v)$, such that

$$-\Delta(u,v) \ \leq f(u,v) + f(v,u) - \tfrac{c(u,v)}{2} \leq \ \Delta(u,v), \tag{5.7}$$

in order to measure the deviation of actual load $(f(u, v) + f(v, u))$ and desired load $(c(u, v)/2)$. This $\Delta(u, v)$ is ideally zero and therefore, the goal is to minimize $\Delta(u, v)$.

This model has the goal to provide a balanced feasible flow on an electrical network by minimizing the distance to half of the capacity. The *flow cost* is the following

$$z(N,f) = \sum_{(u,v)\in A} f(u,v) + \sum_{(u,v)\in A} \Delta(u,v) \tag{5.8}$$

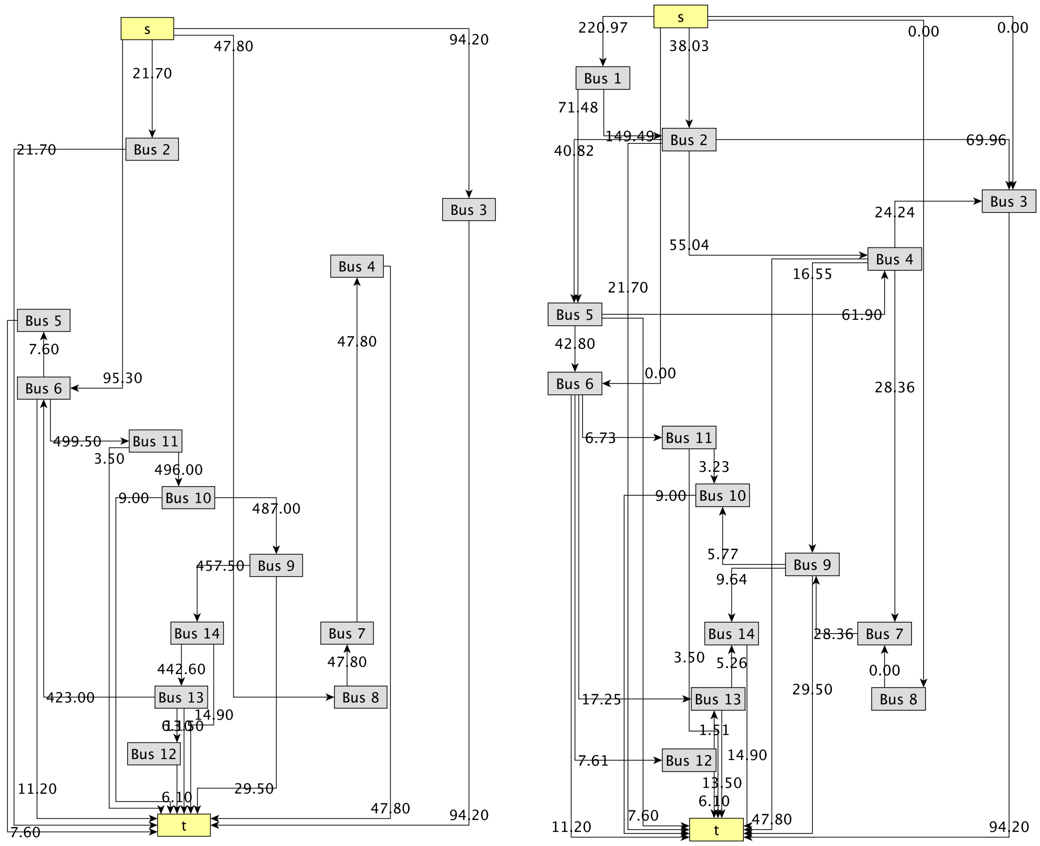

(a) Flow f_{bal} of the balanced flow model in the electrical network N.

(b) Flow f_{opf} of the optimal power flow in the electrical network N.

Figure 5.4.: The electrical network N is the 14-bus network from the Washington University [6]. The helper vertices s (source) and t (sink) are highlighted in yellow.

From Equations 5.2, 5.4, 5.7 and by minimize Equation 5.8, we get a MILP, which we call *balanced MILP* shown in Equation 5.9.

$$
\begin{array}{llll}
\text{minimize} & z(N,f) = \sum\limits_{(u,v)\in A} f(u,v) + \sum\limits_{(u,v)\in A} \Delta(u,v) & & \\
\text{s.t.} & \sum\limits_{v\in V} f(u,v) & = & 0 \\
 & \sum\limits_{u:(s,u)\in A} f(s,u) & = & \sum\limits_{v:(v,t)\in A} c(v,t) \\
 & \sum\limits_{u:(s,u)\in A} f(s,u) - \sum\limits_{v:(v,t)\in A} f(v,t) & = & 0 \\
 & f(u,v) & \leq & c(u,v) \\
 & f(u,v) - y\cdot c(u,v) & \leq & 0 \\
 & f(u,v) + y\cdot c(u,v) & \leq & c(u,v) \\
 & f(u,v)+f(v,u) - \Delta(u,v) & \leq & \frac{c(u,v)}{2} \\
 & f(u,v)+f(v,u) + \Delta(u,v) & \geq & \frac{c(u,v)}{2} \\
 & & & y \in \{0,1\},\ \Delta(u,v) \in \mathbb{R} \\
 & & & f(u,v) \in \mathbb{R}_{\geq 0}\ \forall (u,v)\in A.
\end{array}
\tag{5.9}
$$

Case studies. The goal of the balanced flow model is a power equipartitioning over all edges by minimizing the difference to half of the capacity of each edge (see Equation 5.7).

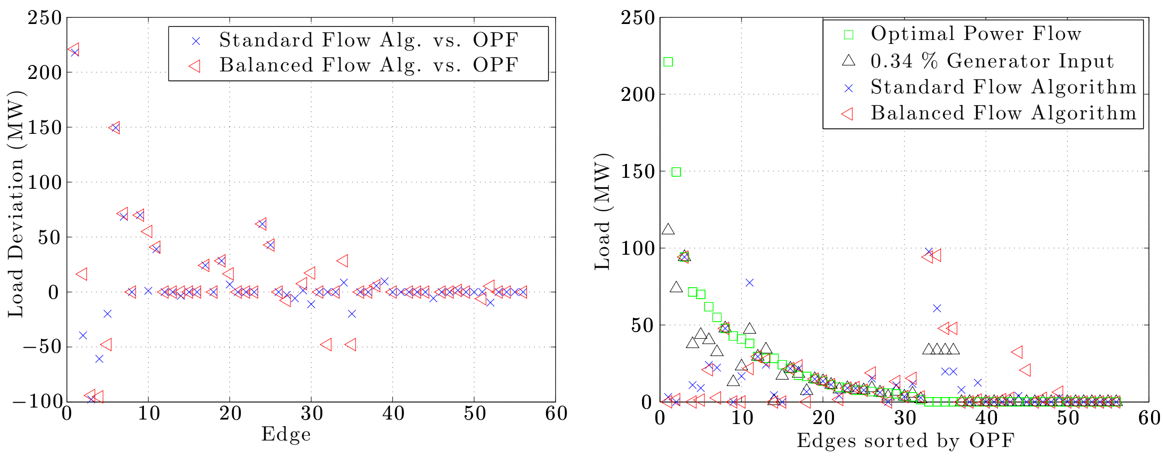

(a) Edge flow deviation between an optimal power flow (OPF) and a balanced flow model including all previous models.

(b) Generator productions of some models are used to calculate a flow using the power flow model on the network N.

Figure 5.5.: Plots for the 14-bus electrical network N from the Washington University [6] concerning the balanced flow model and all previous models.

Furthermore, the flow can only use one direction per vertex pair, which Equation 5.4 describes. Figure 5.4 shows the flow f_{bal} of the balanced flow model (see Figure 5.4a) and f_{opf} of the optimal power flow side by side. Cyclic flows can build possible solutions of the balanced flow model, which can be gathered from Figure 5.4a. There, buses $6-11-10-9-14-13$ form a cycle with a redundant flow of 423.00 MW, which is not realistic.

In Figure 5.5a, the edge deviation is presented. As for the standard flow model the biggest deviation can be found within the first ten edges. The reason is that the generator production for bus 1 is zero MW and therefore the deviation at $e_1 = (s, \text{Bus1})$ is 220.97 MW since the OPF model has a production of 220.97 MW at bus 1. Thus, the missing generator production at bus 1 is distributed over the other generators. From Figure 5.5a we can gather that there are much more edges which differ from the OPF model by using the balanced flow model. The reason is that the balanced flow model attempts to distribute the flow over all edges. In Figure 5.5b we can see the resulting flow of the power flow model by using the generator production of the balanced flow model. It exhibits nearly the same behavior as the standard flow model as the generator production slightly differs.

Overall, the balanced flow model probably provides a more balanced flow in N, but consider in particular all edges. A problem is that there still exist distortions, which can become problematic regarding load peaks in a real network.

As for the standard flow model the production costs are not modeled. Therefore, the balanced flow model has a production cost of 10394 USD, which in comparison with the standard flow model with 10386 USD is worse. But this always depends on the network N and the distribution of the generators. In comparison, the OPF model has costs of 7642 USD.

5.4. Bottleneck Flow Model

Another approach to balance the flow on an electricity network is provided in this section. Again, balancing is done, since the standard flow model produces flows, which are close to the maximum capacity and this leads to faster attrition. In the previous section, the balanced flow provides edges, which are still high charged. In practice and in this thesis, these edges are denoted by bottleneck edges. Bottleneck edges lead to problems in networks, for example line outage, system instabilities and others. In meshed networks like in Germany, there exist fewer bottleneck edges then in non-meshed networks. Due to renewable energies the number of bottleneck edges increases, e.g., ENTSOE indicates that 80% of 100 identified bottlenecks are related to renewable energy resources (RES) [2]. Furthermore, the distance between consumer location and generation location changes, e.g., in France electrical heating is often used, and during winter the generation in France is not sufficient [4]. In this time they also use energy generated in Germany, Poland and Czech Republic. Thus, Germany, especially Baden-Wuerttemberg, serves as energy transfer network [83]. The network of Baden-Wuerttemberg is not designed for such a big load and the number of bottlenecks increases in transfer situations. Even though Germany uses the $k-1$ rule [83] bottlenecks constitute a system vulnerability. Thus, this section prioritize bottleneck edges higher than other edges to archive a lower bottleneck flow within the electricity network. At the beginning, we describe the model and subsequently the experiments are explained to understand possible problems.

The bottleneck flow intends to balance the flow by taking bottleneck edges more into account. The objective function minimizes the maximum edge flow and reduces the flow equally over all edges in the electricity network. This is done iteratively. In each iteration we fix the flow on bottleneck edges with a flow equal to the minimum possible bottleneck flow and reduce the upper bound of all non-fixed edges to that flow. This prevents variations in the maximum flow, since the reduced flow at one bottleneck edge is not shifted to another one as the maximum edge flow correlates with the reduced flow on this bottleneck edge. The flow conservation holds for each vertex and in addition, the edges are limited to a capacity function c. This approach reduces the maximum bottleneck flow and therefore, relieves the edges.

Mathematical model description. We use the same electricity network $N = (G = (V, A), c, s, t)$ as already mentioned in all previous sections. As before, a *feasible flow* f is defined by the flow conservation from Equation 5.1 and capacity constraints from Equation 5.2.

Let N be an electricity network with a feasible flow f. A bottleneck edge e is defined by $f(e) \geq f(e')$ for all $e = (u, v) \in A$. Thus, a balanced flow minimizes the flow on the bottleneck edges to a Δ while reducing the flow equally on all edges. The Δ denotes the smallest possible bottleneck flow (maximum edge flow) in the electricity network and also represents the maximum flow for all observed edges. The *flow cost* for this network is defined by

$$z(N, f, (u, v)) = \Delta \tag{5.10}$$

Now, we iteratively minimize Equation 5.10. In each iteration we get a Δ, which is the minimum of the maximum flow for the current iteration. Furthermore, in each iteration we fix the flow of an arc (u, v), where $f(u, v) = \Delta$, and update the upper bound for all arcs to Δ. This is done for all edges, while prioritizing bottleneck edges, or until Δ is equal to zero. By minimizing the objective function in Equation 5.10, and applying the

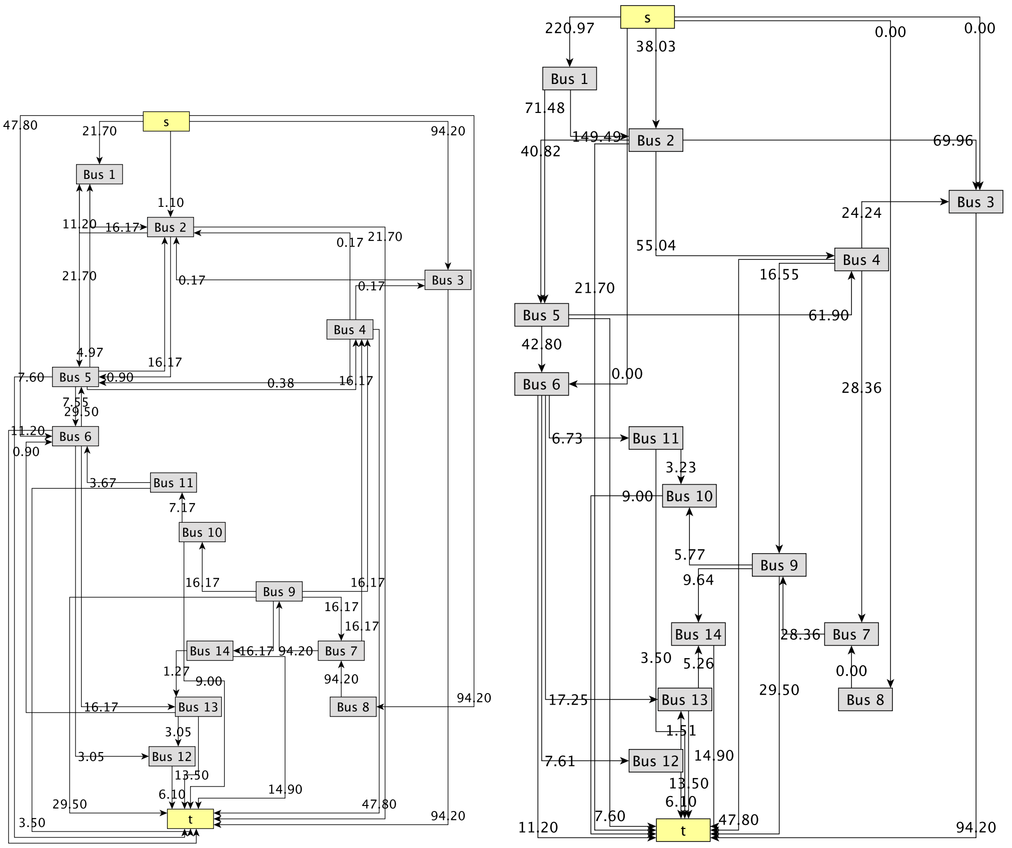

(a) Flow f_{bn} of the bottleneck flow model in the electrical network N.

(b) Flow f_{std} of the optimal power flow in the electrical network N.

Figure 5.6.: The electrical network N is the 14 bus network from the Washington University [6]. The helper vertices s (source) and t (sink) are highlighted in yellow.

constraints from Equations 5.1 and 5.2, we get a LP for one iteration, which we denote as *bottleneck LP*. One iteration is shown in Equation 5.11.

$$
\begin{aligned}
\text{minimize} \quad & z(N,f) = \Delta \\
\text{s.t.} \quad & \Delta - f(u,v) \geq 0 \\
& \sum_{v \in V} f(u,v) = 0 \\
& \sum_{u:(s,u)\in A} f(s,u) = \sum_{v:(v,t)\in A} c(v,t) \\
& \sum_{u:(s,u)\in A} f(s,u) - \sum_{v:(v,t)\in A} f(v,t) = 0 \\
& f(u,v) \leq c(u,v) \\
& f(u,v) \geq 0 \quad \forall (u,v) \in A.
\end{aligned}
\tag{5.11}
$$

Algorithm 5.1 shows such a method to solve the bottleneck flow. We iteratively minimize Equation 5.10.

Case Study. The bottleneck flow f_{bn} is shown in Figure 5.6a and builds another approach to balance a flow on an electrical network N. Instead of minimizing the difference to half of the capacity, this model try to minimize the flow on bottleneck edges. Minimizing the maximum flow on an edge is a iterative LP, which is shown in Algorithm 5.1.

Algorithm 5.1: Solving the MOLP Bottleneck Flow

Data: Vertex set V and edge set E
Result: Flow f

$\mathcal{A}(E_t)$: Solves the bottleneck LP, where Δ is constraint by a set of non-fixed edges E_t and the flow conservation is applied to all fixed and non-fixed edges $(u,v) \in E$
E_t: Set of bottleneck edges
E_t := E
while *is not empty* E_t && Δ != 0 **do**
    $(\Delta, f) = \mathcal{A}(E_t)$
    $(u,v) = find(f(u,v) == \Delta)$
    $E_t = E_t \setminus (u,v)$
end

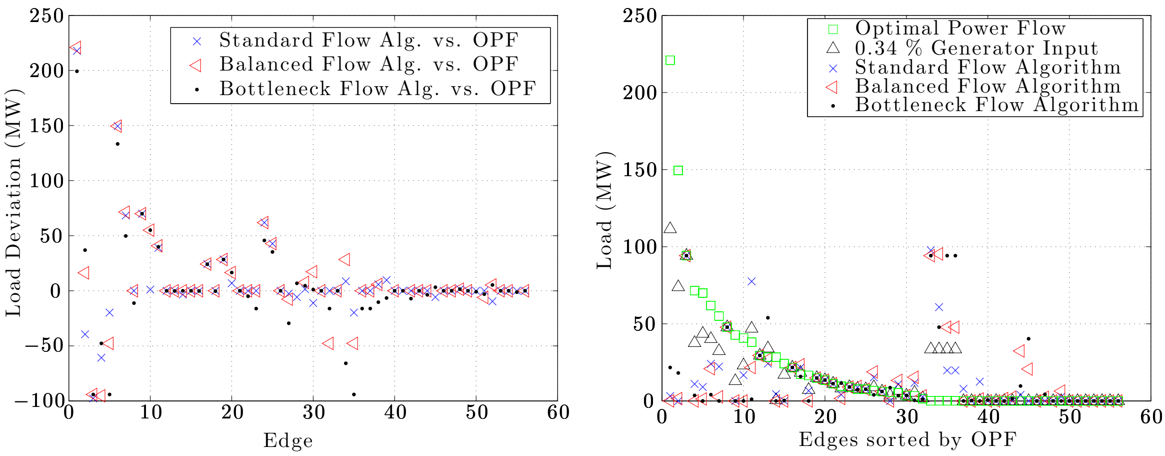

(a) Edge flow deviation between an optimal power flow (OPF) and a bottleneck flow model.

(b) Generator productions of the bottleneck flow model and all previous models are used to calculate a flow using the power flow model on the network N.

Figure 5.7.: Plots for the 14-bus electrical network concerning the balanced flow model and including also the previous standard flow model.

The main deviations are located in the first ten edges, as for the previous models from Sections 5.2 and 5.3. But there exists a distortion at edge e_{35} = (Bus 8, Bus 7) (see Figure 5.7a). Concerning the generators it strikes that the generator at bus 6 is shut down, which is not the case for the balanced flow. This is caused by the order in which Algorithm 5.1 choose the edges.

Comparing both, balancing flow model and bottleneck model, shows that the maximum flow in the electrical network N is minimized by spreading the flow in N, even if both approaches lead to different flows.

For reasons of completeness, the bottleneck flow has production costs of 10121 USD, which is at a reduced rate compared to the previous models. But the production costs depends mostly on the structure of the electricity network and generator distribution in the electricity network, since we do not minimize the generation costs. This model has the focus on the balancing topic.

5.5. Minimum Cost Flow Model

In all previous models we just took care about the flow in an electricity network. We focus on balancing a flow to prevent edges close to the thermal limit. Another important factor are power production costs, which affect the consumer price. This section focuses on a global optimal solution of the total production costs to improve the network efficiency.

Generation costs are strongly dependent on the generation kind, e.g., renewable energy like wind farms and photovoltaic plants (PV), nuclear power plants or fossil power plants. Furthermore, within these different kinds are efficiency differences dependent on the age and other factors [41]. The IEEE data provided by the Washington University [6] does not cover information about generation costs. But by using the method described in Section 4.1, these data are synthetically produced. Thus, we can assume that there is a polynomial cost function for each generator.

In this section, we approximate these polynomial functions to stay linear and show the generator cost functions of the 14 bus system. In addition, the mathematical model is described and some case studies to show missing properties of such a flow.

The idea of this model is to reduce the generator production costs to get an optimal solution. Each generator provides a convex cost function, which we piecewise linear approximate. In addition, the standard flow conservation and the capacity limits are used as already mentioned in the previous sections. The objective function minimizes the generator costs and always selects the right linear function for each interval.

Mathematical model description An electrical network $N = (G = (V, E), c, \gamma, s, t)$ in this model includes an additional function $\gamma : E \to \mathbb{R}_{\geq 0}$ to the previous models, which describes the generator costs, where $\gamma(u, v) = 0$ for $u, v \neq s$. Furthermore, this model works on an undirected graph with edge set E.

Let N be an electrical network and let $f : V \times V \to \mathbb{R}$ be an antisymmetric function, i.e., $f(u, v) = -f(v, u)$ for all $(u, v) \in E$. Thus, f is a *feasible flow* if the flow conservation of Equation 5.1 and capacity constraints from Equation 5.2 are fulfilled.

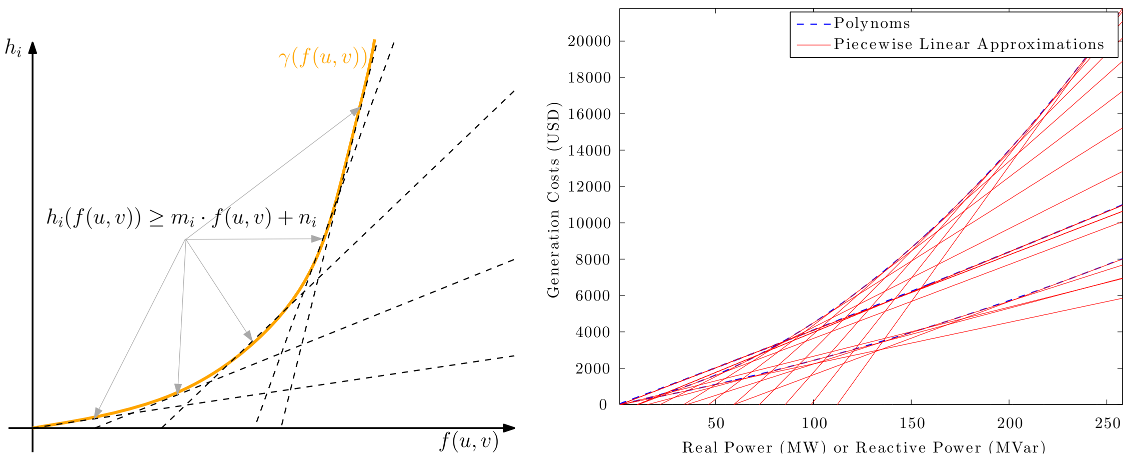

(a) Linear approximation of a function $\gamma(f(u,v))$ is a set H of linear functions, where $h_i \in H$. The topmost section is used by applying $h_i \geq m_i \cdot f(u,v) + n_i$.

(b) Piecewise linear function of the 14-bus network are represented by the red lines and the polynomial is displayed by the gray dashed line.

Figure 5.8.: Visualization of linear approximations.

Algorithm 5.2: Piecewise Linear Approximation

Data: Polynomial γ
Result: Set of linear functions H
load $= \sum_{u:(u,t)\in E} c(u,t)$;
$\mathcal{I} = [0, \text{load}]$; $j = 0$;
for $i = 0$:load **do**
  $m = \left.\frac{d\gamma(x)}{dx}\right|_{x=i}$;
  $b = \gamma(i) - m \cdot i$;
  $\text{scope}_i = (\text{abs}(\mathcal{I}. \cdot m + b - \gamma) \leq \epsilon)$;
  if $|\text{scope}_i| > |\text{scope}_{i-1}|$ **then**
    $H_j = m \cdot x + n$; continue;
  end
  $H_{j++} = m \cdot x + n$;
end

The goal is it to minimize the generation costs over all generators, where n_g is the number of generators $u \in V$, and therefore the *flow costs* for N and function f are defined by

$$z(N, f) = \sum_{v:(s,v)\in E} \gamma(s, v), \tag{5.12}$$

where $\gamma(s, v)$ is the polynomial cost function for generator v.

Piecewise linear approximation. Any continuous function with one variable can be approximated by piecewise linear functions. Therefore, the problem remains linear, since the generator functions are monotone in our case. The maximum approximation error is controlled by a parameter ϵ with

$$|\gamma(x) - h(x)| \leq \epsilon, \tag{5.13}$$

where $\gamma(x)$ (resp., $h(x)$) is the function value of the original function (resp., linear approximated function). The parameter ϵ also determine the number of linear functions for a given function $\gamma(x)$. The set of linear approximations is denoted by H.

Let γ be a continuous function and ϵ be the maximum deviation. Algorithm 5.2 returns a set of linear functions H obtained from γ. The interval for the function γ is set to $\mathcal{I} = [0, \text{load}]$. To maximize the interval for each function $h_i \in H$, Algorithm 5.2 calculates the tangential slope and compares with the previous one by using Equation 5.13. A new scope starts if Equation 5.13 is not fulfilled. By applying Algorithm 5.2 to the generator cost function γ, we get a piecewise linear approximation $h(x)$ of $\gamma(x)$. In Figure 5.8b the linear approximations of the generator costs of the 14 bus network [6] calculated by Algorithm 5.2 is shown.

The goal in this section is to minimize the generation costs for the electrical network N and applying the constraints from Equations 5.1 and 5.2, we get a *minimum cost LP* (shown in Equation 5.14), whose optimal solution is denoted by $\text{OPT}(N) = \min_f z(N, f)$. Furthermore, Figure 5.8a shows how the right linear function is applied for a flow $f(u, v)$. This method is used in Equation 5.14, where it show up as the first constraint, where m

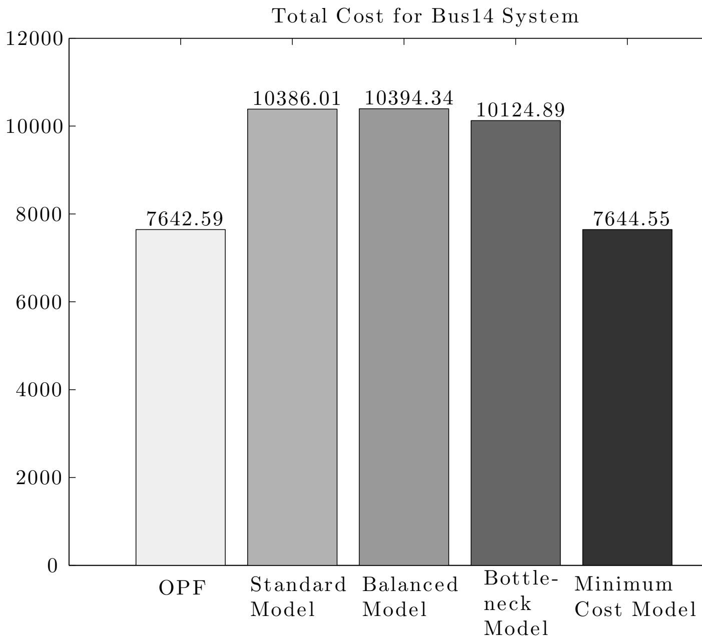

Figure 5.9.: Total power generation cost of all previous models.

is the vector denoting the slope and n the vector denoting the points of intersection with the y-axes for all linear approximations in $h(s,v)$.

$$
\begin{aligned}
\text{minimize } & z(N,f) = \sum_{v:(s,v)\in E} h(s,v) \\
\text{s.t. } & h(s,v) - m \cdot f(u,v) \geq n \\
& \sum_{v\in V} f(u,v) = 0 \\
& \sum_{u:(s,u)\in E} f(s,u) = \sum_{v:(v,t)\in E} c(v,t) \\
& \sum_{u:(s,u)\in E} f(s,u) - \sum_{v:(v,t)\in E} f(v,t) = 0 \\
& f(u,v) \leq c(u,v) \\
& h_i \in \mathbb{R}_{\geq 0},\ f(u,v) \in \mathbb{R}\ \forall (u,v) \in E.
\end{aligned}
\tag{5.14}
$$

Case Studies. The goal of this model was to minimize the generator costs of a network N to achieve an economical result. In all previous models, the generation costs were much higher than for the OPF model. This model provides a solution close to the OPF model, which is shown in Figure 5.9. The reason for the slightly variation is that the linear approximation is not as good as the original generator cost function. But, the problem is still linear.

This model just uses the standard flow model constraints from Section 5.2 to calculate a feasible flow. But it is also possible to combine this model with the balanced or bottleneck flow model from Section 5.3 and 5.4, respectively. Therefore, we see this model as a component, which has to be included in the modeling.

5.6. Combination of Cost Minimization and Balancing

In Sections 5.3 and 5.4, two balancing heuristics were presented. Recall that the reason for this balancing are flows close to the thermal limits of a transmission line. Balancing the flow on transmission lines results in a small flow on highly loaded lines and balancing the generator outputs results in a more spreaded flow in the electrical network. Both together unload bottleneck edges as they spread the generated flow into different subnetworks and lead to a more local flow. Therefore, we use the loss functions of each transmission line to balance the flow and provide a more local spread. In addition, the goal is to minimize the generator production costs. However, balancing the flow can negatively influence the production costs. For a network operator the following is important [56, 11]:

1. Demand and supply meet each other,
2. Satisfy transmission line constraints,
3. Balancing the network and
4. Minimize the generation costs.

Combining such a balancing approach with the minimum cost flow shown in Section 5.5 results in a new model, which is described in this section. We will show a method to combine two problems with a different nature. And, as in the previous sections, we define the mathematical model first and then, we provide a case study for this model.

The idea of this model is to minimize the generator production costs, while balancing the flow in the network. The objective function is weighted with regards to these two goals. To balance the flow in the network we minimize the losses in the network, which reduces the distance between generation and load, since it minimizes the flow costs for each edge. In combination with the minimization of the generation costs, we get a more spread and balanced flow. The flow on bottleneck edge is reduced, since these edges are often placed between two meshed networks. In addition, this model uses the flow conservation and capacity constraints of the previous models and the line loss function is a piecewise linear approximation, which we get by applying the Algorithm 5.2 on this function.

Mathematical model description. In addition to the previous model, an electrical network $N = (G = (V, E), c, \gamma, \ell, B, P_{\text{shift}}, s, t)$ includes—in this model—the loss function ℓ, reverse reactance B and transformer shift angles P_{shift}. Furthermore, $f : V \times V \to \mathbb{R}$ is an antisymmetric function and f is call a *feasible flow* on G if the flow conservation from Equation 5.1 and capacity constraints from Equation 5.2 hold.

The goal of this section is to minimize generation costs and losses to receive a minimal balanced cost flow. The network costs for network N are defined by

$$z_\lambda(N, f) = \sum_{(u,v)\in E} \lambda \cdot \gamma(f(u, v)) + (1 - \lambda)\ell(f(u, v)), \tag{5.15}$$

where $\lambda \in [0, 1]$ denotes the weighting factor.

Combining the objective function of Equation 5.15 with the constraints in Equations 5.1 and 5.2 results in a new model, which we denote as *minimum balanced cost model.*

Case Study. The model has two competing subproblems. Therefore, the weighted sum method [46] is used in this case. This method is called MOLP shown in Section 3.2. Like in Section 5.5 the piecewise linear approximation is used for both functions, generator costs γ and line losses ℓ, to stay linear. To combine the two functions, the problems are weighted against each other by using a weight factor λ. For the experiments it is interesting to get to know how these problems behave by changing the weight λ. The resulting curve corresponds to a Pareto curve as Figure 5.2a suggests. The curve bounds the sample space below.

In Figure 5.10 production costs in USD and losses in MW are shown. If loss costs should be measured in USD/MWh the current energy price can be used, which are in average 0.12 USD/kWh (corresponding to 120 USD/MWh) for domestic consumers or 0.06 USD/kWh (approximately 60 USD/MWh) for industrial consumers in the united

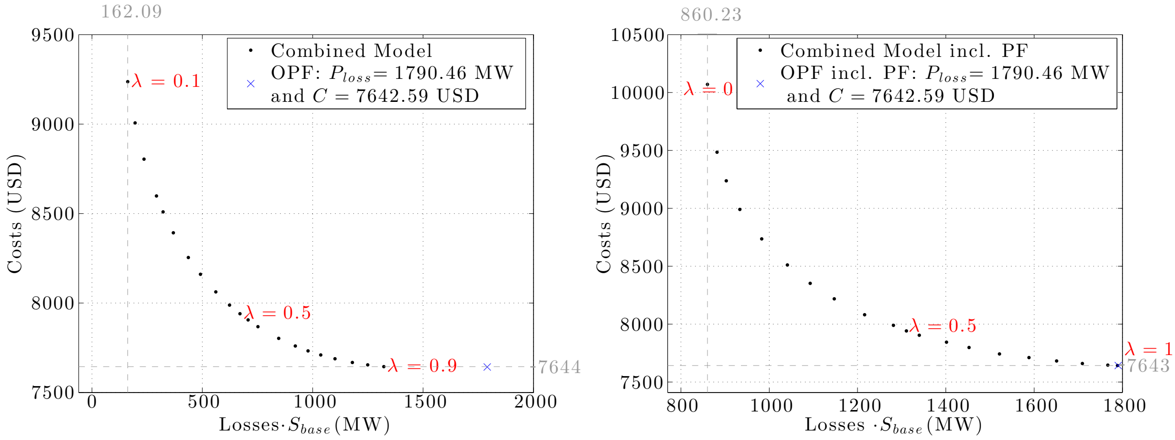

(a) Weighted curve of the combined flow model from $\lambda = 0.1$ to 0.9.

(b) Weighted curve of the combined flow model production included in the power flow model for $\lambda = 0..1$.

Figure 5.10.: The weighted curve appears as Pareto curve, where $\lambda \cdot \gamma + (1 - \lambda) \cdot \ell$.

states [8]. The prices for the European network are available for domestic consumers at Eurostat [9] and for industrial consumers at Eurostat [10]. Another possibility is to use the generation costs for the amount of losses, or stronger use the additional generation costs for the losses. But all variation show, that losses are not negligible.

We do not provide the used methods in Sections 5.2, 5.3 and 5.4 to compare the models with OPF, or include the generator productions into the PF and then comparing it with the OPF, since our focus in this model is to optimize generation costs and line losses. Thus, we compare this model with regards to this two goals.

6. Hybrid Model

The models introduced in Chapter 5 assume that there is a FACTS at each node. This assumption is uneconomical and not practical, because FACTS are currently too expensive [83]. For example, in Germany there is currently only one FACTS (close to Kiel [83]) installed in the transmission network. To create a more realistic model, we define a *hybrid model* that combines the model described in Section 5.6 with the electrical model described in Section 4.3. The hybrid model allows placement of FACTS on a subset of several nodes of the network. A natural question to ask is how many FACTS nodes are necessary in a particular network in order to gain full control over the electricity flow. In particular, in 14-bus system, a small number of FACTS are sufficient to influence the power flow such that it remains optimal.

We start with the mathematical description of the hybrid model. After having shown mathematical properties, we prove different characteristics of this model to understand its possibilities and limits. Within this section, the optimal placement of FACTS is one of the results. At the end of this chapter, we present experiments which also confirm the properties of this model.

6.1. Mathematical Model

The model fusion of the electrical model in Section 4.4 and the flow model from Section 5.6, which includes cost minimization and balancing, is described in this section. In reality, power grids contain a few (expensive) advanced FACTS nodes in combination with existing standard electrical nodes. Thus, we need a flow model that can optimize the power flow in such a hybrid power grid. This mathematical model forms the basis for the next section, where we prove structural properties of this model. We describe the flow conservation in graph theoretical and electrical senses and the scope of both below. In addition, the objective of this model is explained and resembles that of Section 5.6.

As in Section 4.1, an *electricity network* $N = (G, c, \gamma, \ell, B, P_{\text{shift}}, s, t)$ is a graph G with two specified vertices s (source) and t (sink), provided together with functions c, γ, ℓ, B, and P_{shift} on the edges of G, where

- $c : E \to \mathbb{R}_{\geq 0}$ is the edge capacity;
- $\gamma : E \to \mathbb{R}_{\geq 0}$ is the generation cost where $\gamma(u, v) = 0$ if $s \notin \{u, v\}$;
- $\ell : E \to \mathbb{R}_{\geq 0}$ describes the losses, which are defined to be zero for all edges adjacent to s and t;

- $B : E \to \mathbb{R}_{\geq 0}$ is the inverse reactance and
- $P_{\text{shift}} : E \to \mathbb{R}_{\geq 0}$ describes the transformer shift angles.

Graph G is called the *underlying graph* of network N.

Let $V = \{v_1, \ldots, v_n\}$ be the vertex set of G. A *FACTS vector* $x = (x_1, \ldots, x_n) \in \{0, 1\}^n$ is defined as follows:

$$x_i = \begin{cases} 1, & \text{if vertex } v_i \text{ has a FACTS,} \\ 0, & \text{otherwise.} \end{cases} \tag{6.1}$$

We use $F_x = \{v_i \in V : x_i = 1\}$ and $E_x = \{(u, v) \in E : u \in F_x \vee v \in F_x\}$ to denote the subset of FACTS vertices and edges incident to a FACTS vertex *as indicated by* x, respectively. For two FACTS vectors x and y we write $x \leq y$ if and only if $x_i \leq y_i$, for all $i \in \{1, \ldots, n\}$. We use the notation $G(x)$ (resp., $N(x)$) for the graph G (resp., electrical network N), where FACTS are placed as indicated by x.

Let N be an electrical network and let $f : V \times V \to \mathbb{R}$ be an antisymmetric function, i.e., $f(u, v) = -f(v, u)$ for all $\{u, v\} \in E$ and $f(u, v) = f(v, u) = 0$ for all $\{u, v\} \notin E$. Recall that f is called *flow* on G if the following holds:

$$\begin{array}{lll} \sum\limits_{v:\{u,v\} \in E} f(u, v) = 0 & & \forall\, u \in V \setminus \{s, t\} \\ \sum\limits_{u:(s,u) \in E} f(s, u) \;=\; \sum\limits_{v:(v,t) \in E} f(v, t) = \sum\limits_{v:(v,t) \in E} c(v, t) & & \\ f(u, v) \qquad\qquad \leq c(u, v) & & \forall\, \{u, v\} \in E \end{array} \tag{6.2}$$

We say that f is *electrically feasible* for the electrical network $N(x)$, where x is a FACT vector, if there exist phase angles $\Theta(u)$ for all $u \in V \setminus F_x$, such that for each $(u, v) \in E \setminus E_x$:

$$f(u, v) = B(u, v) \cdot (\Theta(u) - \Theta(v)) + P_{\text{shift}}(u, v). \tag{6.3}$$

In this section our goal is to minimize both generation costs and edge losses, so we define the *network cost* for network $N(x)$ and function f to be the following multi-objective function parameterized by a weighting factor $\lambda \in [0, 1]$:

$$z_\lambda(N(x), f) = \sum_{(u,v) \in E} \lambda \cdot \gamma(u, v) + (1 - \lambda) \cdot \ell(u, v) \tag{6.4}$$

Given a network $N(x)$ for a FACTS vector x, Equation 6.2 and Equation 6.3 together with the objective function given by Equation 6.4, which we seek to minimize, comprise a MOLP (which we will refer to as *Hybrid-MOLP*) with f and Θ being variable vectors. A feasible solution of such a MOLP is shortly denoted by $s = (f, \Theta)$ and the value of an optimal solution for a fixed parameter λ by $\text{OPT}(N(x), \lambda) = \min_f z_\lambda(N(x), f)$.

6.2. Mathematical Properties

From Zeitler [83] we know that FACTS are expensive. Thus, it is interesting to know if the solution improves by increasing the number of FACTS and where the best placement of FACTS is. By exploiting the structure of an electrical network it may be possible determine the minimum number of FACTS that are needed for an optimal solution. Therefore, we prove several properties of electrical networks in the following.

First of all, we want to know if a feasible solution in an electrical network with a FACTS vector x_i also provides a solution in the same electrical network with a FACTS vector x_{i+1}, where $x_{i+1} \geq x_i$. This is crucial, since it would otherwise it become problematic to show that the quality of the solution improves by increasing number of FACTS.

Lemma 1. Let N be an electrical network and let $x \leq y$ be two FACTS vectors. If $f : V \times V \to \mathbb{R}$ is an electrically feasible function for $N(x)$, then it is also an electrically feasible function for $N(y)$.

Proof. Let $\Theta_x(u)$ be the transformer shift angles for $N(x)$. Since we know $x \leq y$, it follows that $F_x \subseteq F_y$, $E_x \subseteq E_y$. We define $\Theta_y(u) := \Theta_x(u)$ for $u \in V \setminus F_y$. Therefore, $E \setminus E_y \subseteq E \setminus E_x$ and $f|_{E\setminus E_y}(u,v) = f(u,v)$ for all $(u,v) \in E \setminus E_y$, which, together with the definition of electrical feasibility (see Equation 6.3), shows that f is an electrically feasible function for $N(y)$. □

This shows that a solution remains feasible by increasing the number of FACTS in an electrical network and therefore the solution for a of FACTS vector x is at least as good as the solution for a FACTS vector $y \leq x$ in an electrical network. The result helps us to prove the monotonic behavior of $z_\lambda(N(x), f)$.

Consider a Hybrid-MOLP for the electrical network $N(x)$ (resp., $N(y)$) called MOLP$_\mathcal{A}$ (resp., MOLP$_\mathcal{B}$) and let $\mathcal{A}$ (resp., $\mathcal{B}$) be the set of feasible solutions for MOLP$_\mathcal{A}$ (resp., MOLP$_\mathcal{B}$). Let $s = (f, \Theta) \in \mathcal{A}$. As a solution for MOLP$_\mathcal{A}$, f and Θ fulfill Equations 6.2 and 6.3. From the latter it follows that f is electrically feasible for $N(x)$ with phase angles Θ. Therefore, by Lemma 1, f is electrically feasible for $N(y)$. Since f is a flow in $N(x)$, (Equation 6.2 fulfilled) it is also a flow in $N(y)$, and therefore s is a feasible solution for MOLP$_\mathcal{B}$, i.e., $s \in \mathcal{B}$. This proves that $\mathcal{A} \subseteq \mathcal{B}$, and therefore, the following corollary holds.

Corollary 2. Let N be an electrical network and let x and y be two FACTS vectors with $x \leq y$. Then it holds that $\text{OPT}(N(y), \lambda) \leq \text{OPT}(N(x), \lambda)$ for all $\lambda \in [0, 1]$.

From Corollary 2 it follows that adding more FACTS to any FACTS vector provides an improved or equal solution. Now we know that it could make sense to include FACTS in an electrical network, because the solution may improve.

It is interesting to see when the solution improves with the number of FACTS. From Section 5.1 we know that a FACTS vertex influences incoming and outgoing edges. Therefore, a vertex cover is sufficient to get the same optimal solution as for the electrical network with FACTS on all vertices. A *vertex cover* is a set where each edge of N is incident to at least one vertex in the vertex cover set. In the following, we explain some notation that is used for the next steps.

Let $N = (G = (V, E), c, \gamma, \ell, B, P_{\text{shift}}, s, t)$ be an electrical network and $V' \subseteq V$. Then $N[V'] = N' = (G' = (V', E'), c', \gamma', \ell', B', P'_{\text{shift}}, s, t)$ is the *subnetwork of* N induced by V', denoted by $N' \sqsubseteq N$, with $V' \subseteq V$, $E' \subseteq E$ and the functions implicitly restricted to G'.

Let x be a FACTS vector. A *FACTSless electrical network* $N' = (G' = (V', E'), c', \gamma', \ell', B', P'_{\text{shift}}, s, t)$ of $N(x)$ is a subnetwork $N' \sqsubseteq N$ induced by vertices V', where $V' \subseteq V \setminus F_x$ and $E' \subseteq E \setminus E_x$.

Let $C = \{v_1, \ldots, v_l\}$ be a set of *cut vertices*, which split the network into a set of blocks $\mathcal{H} = \{H_1, \ldots, H_k\}$, where $V_i \subset V$ denotes the set of vertices in H_i and $E_i \subset E$ is analogously defined. The restriction of an antisymmetric function to block H_i is denoted by $f_i := f|_{H_i}$.

Lemma 3. Let N be a FACTSless network and let $v \in V$ be a vertex in the underlying graph. Then N has an electrically feasible function if and only if it has an electrically feasible function with $\Theta(v) = c$ for an arbitrary constant c.

Proof. Let f be an electrically feasible function in N with $\Theta(u)$ for all $u \in V$, such that Equation 6.3 holds. Let c be an arbitrary constant and $\Theta'(v) = c$ the new value of $\Theta(v)$.

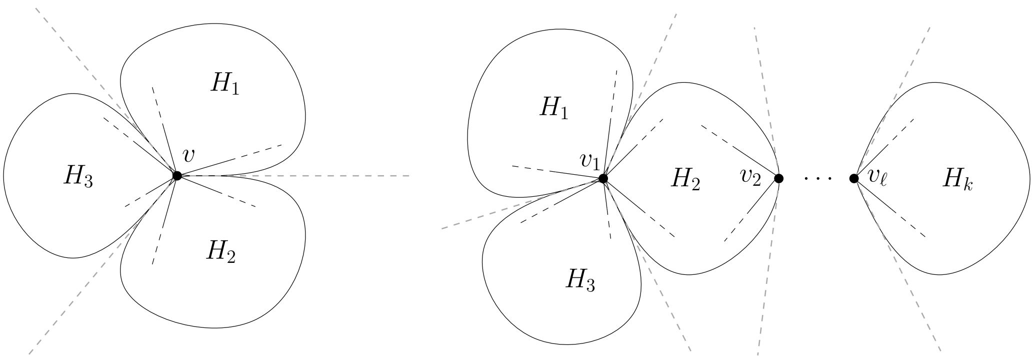

(a) A cut vertex v splits the network N into three blocks H_1, H_2 and H_3.

(b) A set of cut vertices $C = \{v_1, \ldots, v_\ell\}$ split the network N into a set of blocks $\mathcal{H} = \{H_1, \ldots, H_k\}$.

Figure 6.1.: Cut vertices splitting the network N into blocks. The gray dashed lines represent the curves, where we split the network into components. Each block is a subnetwork itself and includes the cut vertices.

Furthermore, define $\Delta = \Theta(v) - c$. We set the values of $\Theta'(u) = \Theta(u) - \Delta$ for all $u \in V \setminus v$ such that there is a new assignment, which implies the following:

$$
\begin{aligned}
& f(u,v) = B(u,v) \cdot (\Theta'(u) - \Theta'(v)) + P(u,v) \\
\Leftrightarrow\quad & f(u,v) = B(u,v) \cdot (\Theta(u) - \Delta - (\Theta(v) - \Delta)) + P(u,v) \\
\Leftrightarrow\quad & f(u,v) = B(u,v) \cdot (\Theta(u) - \Theta(v)) + P(u,v)
\end{aligned} \tag{6.5}
$$

This proves that setting $\Theta(v)$ to an arbitrary constant c, such that $\Theta'(v) = c$ results in a new assignment of $\Theta'(u)$ for all $u \in V \setminus v$, which fulfill Equation 6.3 and therefore, the same function f is electrically feasible for this new assignment Θ'.

The other direction follows immediately. □

Consider a FACTSless network N, a cut vertex $v \in V$, an electrically feasible function f in N and a set of cut vertex blocks $H_1, \ldots, H_k$ for v shown in Figure 6.1a. By cutting the network at v, the assignment of $\Theta_i(u)$ for $u \in V_i$ remains as in N. This results in an electrically feasible function f_i in H_i, for $i = 1, \ldots, k$, as there are no changes with respect to Equation 6.3.

This will be expand to a cut vertex with blocks in an electrical network N to get a more general assumption.

Let v be a cut vertex in G and $\mathcal{H} = \{H_1, \ldots, H_k\}$ be the set of induced blocks (see Figure 6.1a). Let $f_1, \ldots, f_k$ be electrically feasible functions in $H_1, \ldots, H_k$, respectively. Connecting blocks $H_1, \ldots, H_k$ by identifying all copies of v yield the original network N. From Lemma 3 it follows that choosing an arbitrary constant for $\Theta(v) = c$ results in an electrically feasible function in each block i with $\Theta_i(u) = \Theta_i(u) - \Delta_i$, where $\Delta_i = \Theta_i(v) - c$. As we connect the blocks in v with $\Theta(v) = c$ and since each block has an electrical feasible function, this results in an electrically feasible function f in N. Thus, the following corollary holds.

Corollary 4. *Let N be a FACTSless network and let $v \in V$ be a cut vertex yielding a set of blocks $\mathcal{H} = \{H_1, \ldots, H_k\}$ in N. Then there is an electrically feasible function f in N if and only if there are electrically feasible functions f_i in H_i, for each $i = 1, \ldots, k$.*

By applying Corollary 4 recursively on a set of cut vertices C (see Figure 6.1b), we get an electrically feasible function in each block H_i, which together results in an electrically feasible function f in N, and thus Corollary 5 holds.

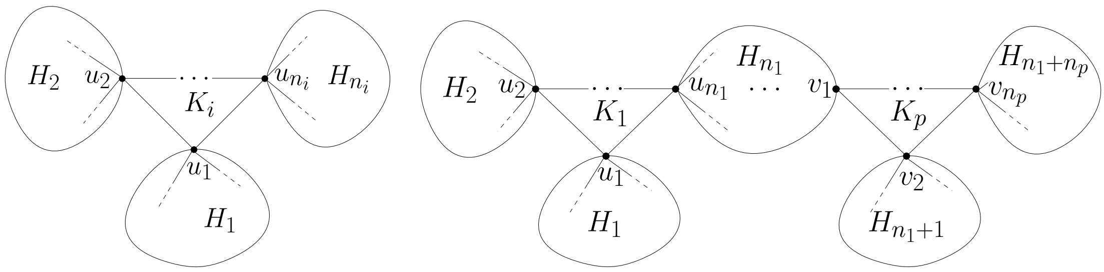

(a) A cycle K_i splits the network N into blocks H_1, H_2 and H_{n_i}.

(b) A set of cycles $\mathcal{K} = \{K_1, \dots, K_p\}$ splits the network into multiple blocks.

Figure 6.4.: Cycles where an edge is only covered on one cycle, split the network N into a set of blocks H. Each block is a subnetwork itself and could cover a cycle again.

Corollary 5. Let N be a FACTSless network, let $C = \{v_1, \dots, v_\ell\} \in V$ be a set of cut vertices with a set of blocks $\mathcal{H} = \{H_1, \dots, H_k\}$ in N. Then there is an electrically feasible function f in N if and only if there is an electrically feasible function f_i in H_i for each $i = 1, \dots, k$.

Let $\mathcal{K} = \{K_1, \dots, K_p\}$ be a set of cycles in G. Recall that f is an antisymmetric function in N. We define $f_i = f|_{K_i}$ as an antisymmetric function on cycle K_i, where V_i is the vertex set of K_i with cardinality $n_i = |V_i|$.

Let f' be a flow on a subgraph $G' = (V', E')$ and $K_i = (v_1, \dots, v_k)$ a cycle in G'. The *maximum cyclic flow* x_i is defined as $x_i \equiv \max\{0, \min\{f(v_1, v_2), f(v_2, v_3), \dots, f(v_k, v_1)\}\} + \min\{0, \max\{f(v_1, v_2), f(v_2, v_3), \dots, f(v_k, v_1)\}\}$. That is, a maximum cyclic flow is a redundant flow and subtracting x_i from the flow f_i results in at least one edge having a flow equal to zero. In Figure 6.2, an example of a maximum cyclic flow is shown, where the cyclic flow is $x \equiv 3$.

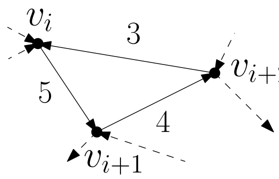

Figure 6.2.: A cycle with a maximum cyclic flow of $x \equiv 3$.

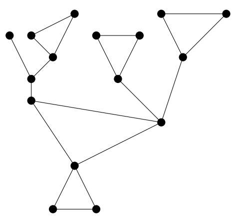

Figure 6.3.: A cactus.

In graph theory a *cactus* is a connected graph G, where two cycles have at most one common vertex. In particular, removing one edge from every cycle in G results in a tree. Every block H_i is either an edge or a cycle. Figure 6.3 shows a cactus with five cycles and ten blocks H_i. It shows that the cycles are either connected via a vertex, an edge or a path of edges. In particular, cycles never share an edge.

Lemma 6. Let N be a FACTSless network whose underlying graph G is a cactus, including a set of cycles $\mathcal{K} = \{K_1, \dots, K_p\}$ with infinite capacity on the edges of those cycles. Then a function f in N is an electrically feasible flow if and only if $f_i - x_i$ is an electrically feasible flow in K_i, where x_i denotes the cyclic flow.

Proof. Let f be a feasible flow in N and let $\mathcal{K} = \{K_1, \dots, K_p\}$ be the set of all cycles in N. We consider a cycle K_i with vertices $V_i = \{u_1, \dots, u_{n_i}\}$ (see Figure 6.4a). From Equation 6.3 and the cyclic flow for cycle K_i we obtain:

$$\begin{pmatrix} B(u_1,u_2) & -B(u_1,u_2) & 0 & \dots & & -1 \\ 0 & B(u_2,u_3) & -B(u_2,u_3) & \dots & & -1 \\ \vdots & & \ddots & & & \vdots \\ -B(u_{n_i},u_1) & & \dots & & B(u_{n_i},u_1) & -1 \end{pmatrix} \cdot \begin{pmatrix} \Theta(u_1) \\ \Theta(u_2) \\ \vdots \\ \Theta(u_{n_i}) \\ x_i \end{pmatrix} = (f_i) - (P_{\text{shift}_i}), \tag{6.6}$$

where x_i is the cyclic flow on K_i, (f_i) and (P_{shift_i}) are row vectors with $(f_i) = (f_i(u_1,u_2), f_i(u_2,u_3), \dots, f_i(u_{n_i},u_1))$ and $(P_{\text{shift}_i}) = (P_{\text{shift}_i}(u_1,u_2), P_{\text{shift}_i}(u_2,u_3), \dots, P_{\text{shift}_i}(u_{n_i},u_1))$ for all $j = 1, \dots, n_i$. By applying the Gaussian elimination method, the matrix in Equation 6.6 is in row echelon form and the last line is reduced to

$$-\left(\sum_{j=1}^{n_i-1} \frac{B(u_{n_i},B_{u_1})}{B(u_j,u_{j+1})} + 1\right) x_i = f_i(u_{n_i},u_1) + \sum_{j=1}^{n_i-1} \left((f_i(u_j,u_{j+1}) - P_{\text{shift}_i}(u_j,u_{j+1})) \cdot \frac{B(u_{n_i},B_{u_1})}{B(u_j,u_{j+1})}\right) \tag{6.7}$$

This shows that Equation 6.6 is a linear independent equation system and therefore there exist solutions for $\Theta(u_i)$ for all $u_i \in V_i$ for the value x_i from Equation 6.7. In addition, we can freely choose one $\Theta(u_i)$ value in K_i, since we have $n-1$ constraints on n variables.

As we look at a single cycle K_i in N there are vertices where the incoming flow or outgoing flow is bigger. To achieve the conservation of flow we set vertices with more outgoing (resp., incoming) then incoming (resp., outgoing) flow to be a source (resp., sink).

This shows that there exists an electrically feasible function in K_i. If f is a flow, then the capacity constrain for a given capacity c_i has to hold, that is

$$x_i + f_i \leq c_i. \tag{6.8}$$

As the capacity on cycles is set to infinity Equation 6.8 holds by assumption.

Consider that each cycle K_i is a block denoted by H_i and each block is connected via a cut vertex u_i to the other blocks (see Figure 6.4). Then we can directly apply Corollary 5, such that there exists an electrically feasible assignment of phase angles in H_i for an arbitrary $\Theta(u_i)$, for each $i = 1, \dots, n_i$. Thus, f_i does not change the flow of the other blocks, and therefore there exists an electrically feasible flow in N. □

Lemma 6 has some limitations. First of all, consider a cycle K_i with three vertices u, v and w in V_i. Furthermore, we set $P_{\text{shift}} = 0$ and $B_{(u,v)} = 1$ for each $u, v \in V_i$. Then, from Equation 6.6 we obtain:

$$\begin{aligned} \Theta(u) - \Theta(v) - x &= f_1, \\ \Theta(v) - \Theta(w) - x &= f_2, \\ \Theta(w) - \Theta(u) - x &= f_3. \end{aligned} \tag{6.9}$$

It follows that $x = -1/3(f_1+f_2+f_3)$. By setting the flow f_i equally to the capacities, then adding the cyclic flow x to the flow f_i, we get a capacity exceedance. This is the reason for setting the capacities in Lemma 6 to infinity. In addition, adding a cyclic flow increases the line losses, which have a direct influence to the total flow costs z_λ, and therefore the solution is not optimal anymore.

6.3. Structural Findings

In the previous section, we examined the properties of a hybrid model. Since FACTS are expensive, these properties are used to determine the optimal placement of FACTS in an electricity network to reach an optimal flow. We show that a flow is controllable in tree and cactus structures, which are used to determine the placement of FACTS.

We first decided to put FACTS everywhere to control the whole flow in the electricity network in order to reach an optimal solution (see Chapter 5). This, however, is uneconomical for the network operator, and therefore we developed the hybrid model. In Section 6.2, we show that a placement of FACTS with regards to a vertex cover set is sufficient to control the whole flow in the electricity network and to reach an optimal flow in N. Furthermore, using the definition of flow from Section 6.2, from Corollary 5 the following theorem follows:

Theorem 1. Let $N = (G = (V, E), c, \gamma, \ell, B, P_{\text{shift}}, s, t)$ be a FACTSless network, whose underlying graph is a tree. For any flow f on N there exists phase angles $\Theta : V \to \mathbb{R}$, such that f is an electrically feasible flow.

Definition 1. Two flow functions f and f' are called equivalent if they differ by a set of cyclic flows.

From Lemma 6 we get the next theorem.

Theorem 2. Let $N = (G = (V, E), c, \gamma, \ell, B, P_{\text{shift}}, s, t)$ be a FACTSless network, whose underlying graph is a cactus, where $c = \infty$ on all cycle edges. For any flow f, exists $\Theta : V \to \mathbb{R}$, such that there exists an electrically feasible flow f' on N which is equivalent to f.

Definition 2 (Feedback Vertex Set)**.** A feedback vertex set V' in $N = (G = (V, E), c, \gamma, \ell, B, P_{\text{shift}}, s, t)$ is a set of vertices $V' \subseteq V$ such that $N[V \setminus V']$ is a forest in N.

By applying Theorem 1 the following theorem holds:

Theorem 3. Let $N = (G = (V, E), c, \gamma, \ell, B, P_{\text{shift}}, s, t)$ be an arbitrary electrical network and let $V' \subset V$ be a feedback vertex set of G. Assume that FACTS are placed at all the nodes of V'. Then any flow on N is an electrically feasible flow.

One can seek to find the minimum feedback vertex set, however this is NP-hard [48].

6.4. Case Study

The hybrid model combines the electrical model with the balanced cost flow model from Section 5.6. As in the previous model our goal is to minimize transmission line losses and generation costs. For each FACTS vectors, we get a Pareto curve similar to those in Section 5.6, where FACTS are placed on all vertices. Figure 6.5 displays the behavior for a specific weighting factor λ (here $\lambda = 0.5$) and all possible FACTS vectors for the 14-bus network, which are in total $2^{14} - 1$ different FACTS vectors allocations with different total flow costs z_λ.

In Figure 6.5a, the magenta lines denote the lines with the same total flow costs z_λ. The optimal value for z_λ is given by x_n, where FACTS vector x_n describes an electrical network with FACTS on every vertex. The worst value for z_λ provides FACTS vector x_1 without FACTS. Vertices s (source) and t (sink) are always FACTS, as they control the total generation and load (see Section 5.1). This approves the monotonical properties of the

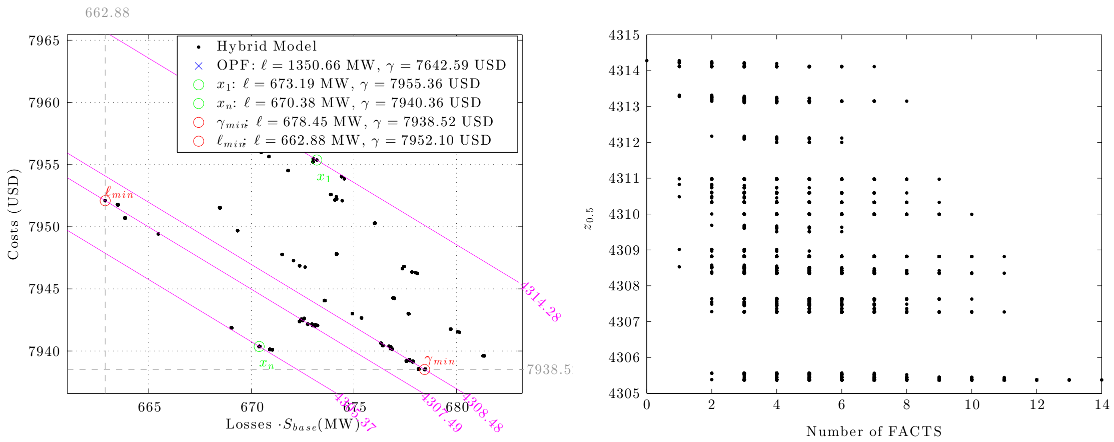

(a) Losses in MW and costs in USD of all possible FACTS vectors for $\lambda = 0.5$.

(b) Distribution of function values z_λ for different quantities of FACTS of all possible FACTS vectors for $\lambda = 0.5$.

Figure 6.5.: The number of FACTS determine the quality of the solution. Therefore, the 14 bus network is used to visualize the monotonicity of the solution space and the number of FACTS, which results in a good solution.

hybrid model with regards to x_1 and x_n from Corollary 2. In Lemma 1 and Corollary 2 we proved that an increasing number of FACTS results in a better or equally good solution for z_λ as with less FACTS. Furthermore, the FACTS vector with the lowest loss value (resp., cost value) is marked with $\ell_{\min}$ (resp., $\gamma_{\min}$). Thus, for a specific weight factor λ, the values are bounded below by three functions $f_{\ell_{\min}}$, $f_{\gamma_{\min}}$ and $f_{\min\ z_\lambda}$, which describe the same minimum losses, minimum costs and minimum function values of the hybrid model, respectively.

In Figure 6.5b the FACTS vectors with the same FACTS quantity are listed at the same vertical line. From Figure 6.5b it can be extracted that four FACTS—if placed at the right nodes—for the 14 bus network are sufficient to get an approximately equally good result as for the electrical network with FACTS on all vertices. Thus, the structure of the network and the right positioning of FACTS is not irrelevant to achieve an optimal flow in the network, which we already mentioned in Lemmas and Corollaries 3 to 6.

In the example data sets from the Washington University [6], some edges have a resistance equal to zero. Thus, the costs for line losses are for each flow on these lines equal to zero. This causes cyclic flows up to the maximum capacity. To prevent cyclic flows in an electrical network, edges with a resistance equal to zero are set to ϵ. The plots in Figure 6.5 using these changed resistance data, and thus have slightly higher values than using the original data. The optimal power flow result has higher losses and for scaling reasons it is just mentioned in the legend for reference.

7. Conclusion

In this thesis, we studied how classical methods for the calculation of flow in networks can be adapted to the calculation of power flows in electricity networks. While methods for the calculation of power flow in electricity networks have been improved over decades, classical flow algorithms have not been utilized due to multiple differences in the nature of usual flow and power flow.

In the beginning of this thesis, we tried to understand basic functional operations of electricity network. Afterwards, we considered graph-theoretical methods in electricity networks and presented two approaches: The first approach used the generator productions of flow models as input for the power flow (PF) method in order to obtain an electrical flow. We made use of different heuristics to get a better generator production. The second approach considered FACTS at each node of the electricity network. This gave us the possibility to apply classical flow methods to compute the power flow in electricity networks. The flow produced this way was unbalanced, thus some branches were much heavier used than the others. We considered two heuristics to produce a more balanced flow. The first one balanced all edges to half of the capacity, while the second one prioritized bottleneck edges. These heuristics resulted in worse generator production costs in comparison to the OPF method. Thus, as a next step, we minimized the generator cost functions, which resulted in optimal generation costs, however the flow was still unbalanced. We therefore combined the two objectives, generation costs and balancing, which was done by minimizing the weighted sum of generator costs and line losses. This model yielded good results regarding the combination of generator costs and balancing. Motivated by the fact that placing FACTS at every node is too expensive, we introduced a hybrid flow model for networks containing nodes with and without FACTS. This model integrated the PF method into the model which minimizes both generation cost and losses. Finally, we proved several theoretical properties of networks containing nodes with and without FACTS. In particular, we described the set of nodes where FACTS have to placed such that the electrical flow can be found using only a classical flow computation method.

The initial target of this work was to improve the efficiency of power flow calculation. The models we have developed are based on calculations of flow in networks; a task for which efficient algorithms exist. Thus, we expected that the developed models perform better than the classical methods for power flow calculation, which include the solving of non-linear optimization problems. Testing the efficiency of our models is one of the future research directions.

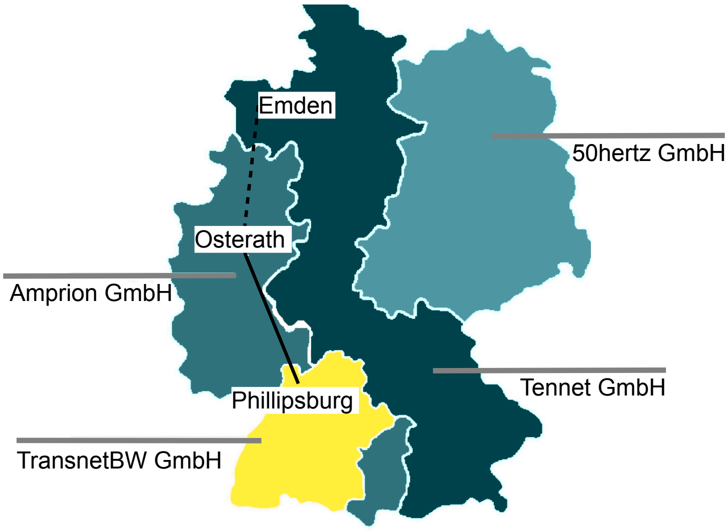

Figure 7.1.: The planned HVDC transmission line expansion in Germany from [12, 13] to improve the integration of the offshore wind farms and other renewable energy plants. The black consecutive line represents the plant *ULTRA-NET*.

In the future, it would be interesting to optimize more than just production costs and losses in electricity networks. Thus, possible research directions include failure analysis and optimization of the structure of electricity networks. Furthermore, we know from TransnetBW [12, 13, 83], that the energy produced by offshore wind farms in Northern Germany should be distributed over the country, since the energy consumed is not as high as the energy produced in this region. There are projects which construct new *high voltage direct current* (HVDC) transmission lines from the north to the south of Germany (for example, the ULTRANET in Figure 7.1). In this context, optimizing the energy distribution in an AC electricity network containing HVDC transmission lines, as well as optimizing the construction of those transmission lines open up further possible areas of research.

8. Appendix

A. 30-Bus Electricity Network

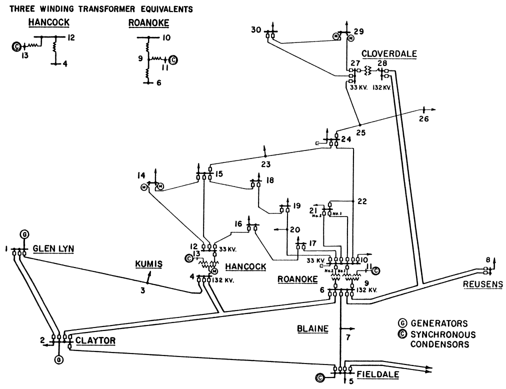

Figure A.1.: A 30-bus electricity network from the University of Washington [6].

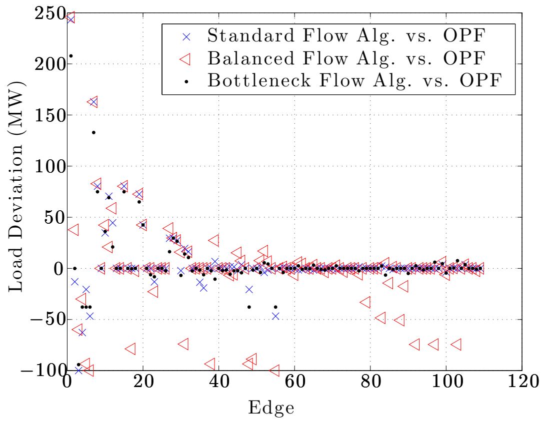

(a) Edge flow deviation between an optimal power flow (OPF) and the graph theoretical flow models.

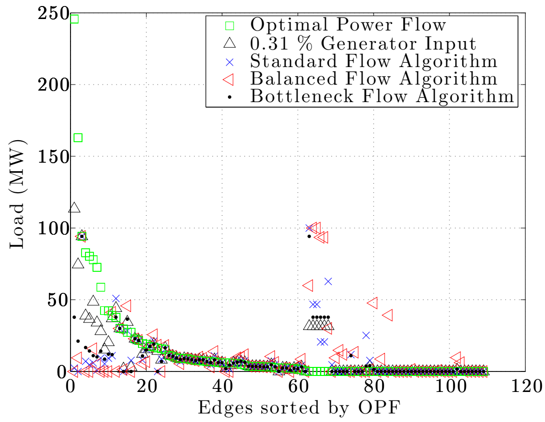

(b) Generator productions of the graph theoretical flow models are used to calculate an electrical flow using the power flow (PF) method. The edges are decreasingly sorted by the OPF flow on the edges.

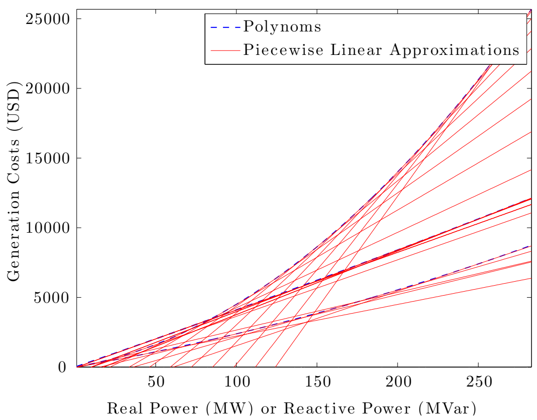

(c) Piecewise linear generator cost functions of the 30-bus network are presented by the red lines and the polynomial is displayed by the gray dashed line.

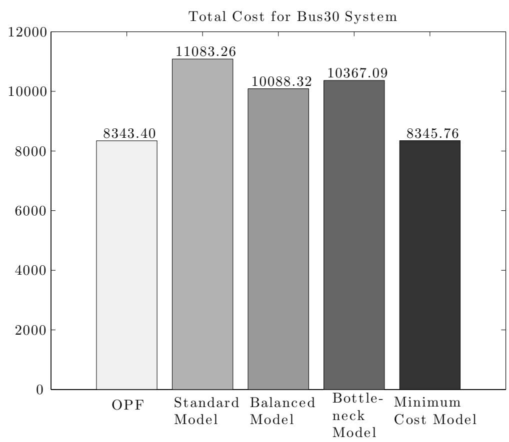

(d) Total power generation cost of all simple weighted flow models of this thesis.

Figure A.2.: Plots for the 30-bus electricity network.

B. 57-Bus Electricity Network

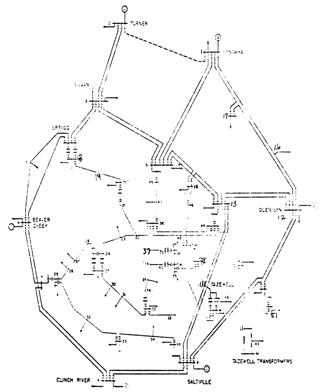

Figure B.3.: A 57-bus electricity network from the University of Washington [6].

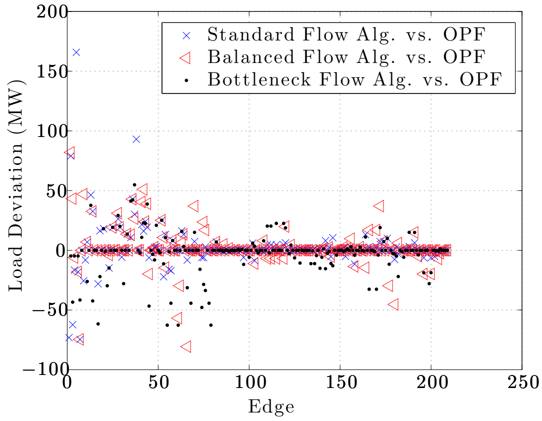

(a) Edge flow deviation between an optimal power flow (OPF) and the graph theoretical flow models.

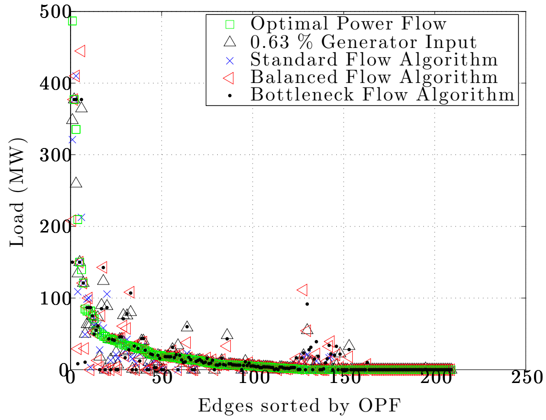

(b) Generator productions of the graph theoretical flow models are used to calculate an electrical flow using the power flow (PF) method. The edges are decreasingly sorted by the OPF flow on the edges.

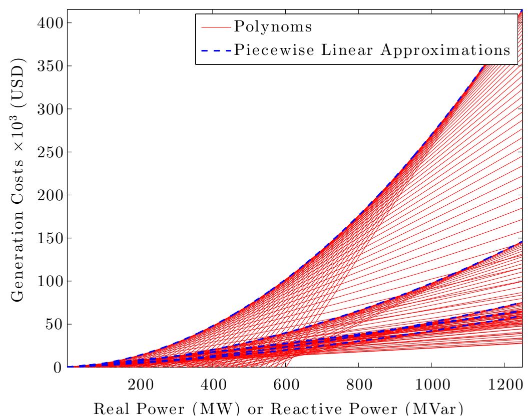

(c) Piecewise linear generator cost functions of the 57-bus network are presented by the red lines and the polynomial is displayed by the gray dashed line.

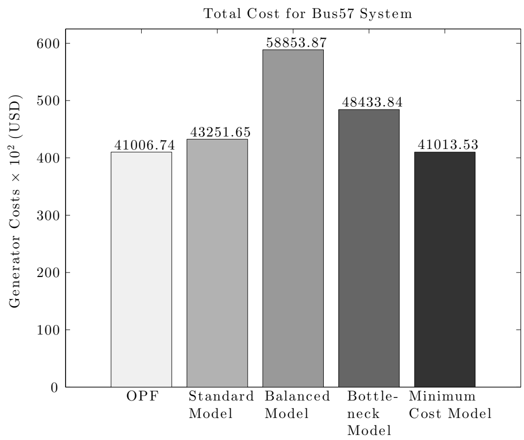

(d) Total power generation cost of all simple weighted flow models of this thesis.

Figure B.4.: Plots for the 57-bus electricity network.

C. 118-Bus Electricity Network

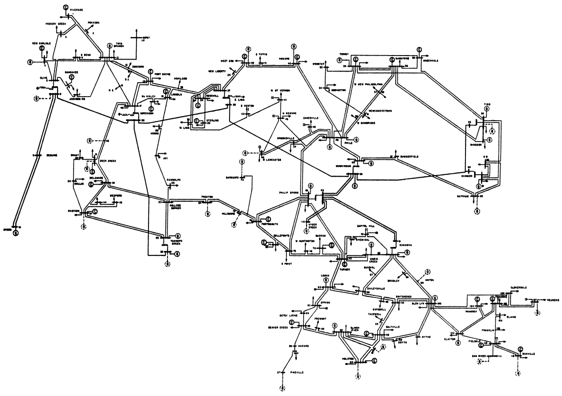

Figure C.5.: A 118-bus electricity network from the University of Washington [6].

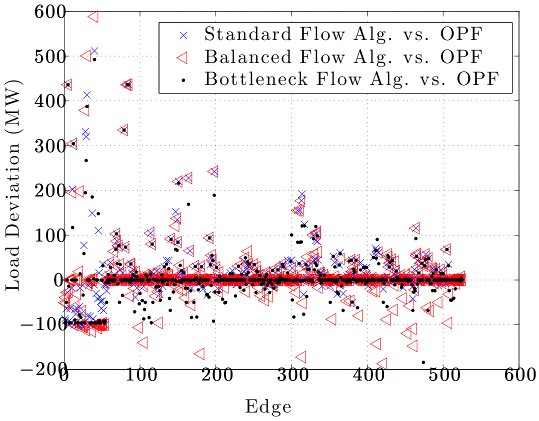

(a) Edge flow deviation between an optimal power flow (OPF) and the graph theoretical flow models.

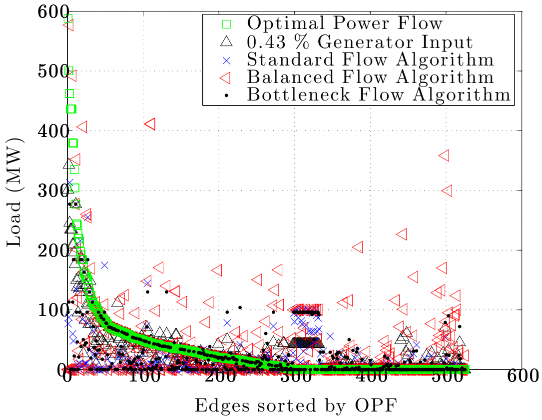

(b) Generator productions of the graph theoretical flow models are used to calculate an electrical flow using the power flow (PF) method. The edges are decreasingly sorted by the OPF flow on the edges.

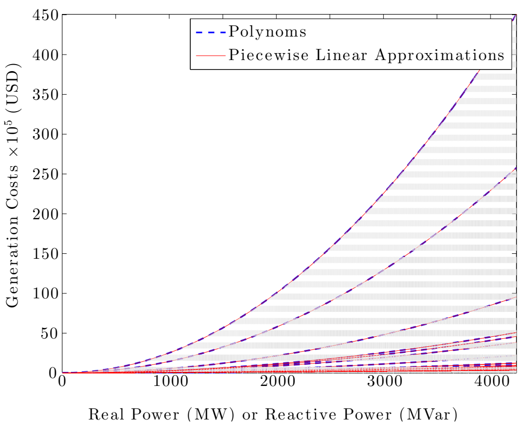

(c) Piecewise linear generator cost functions of the 118-bus network are presented by the red lines and the polynomial is displayed by the gray dashed line.

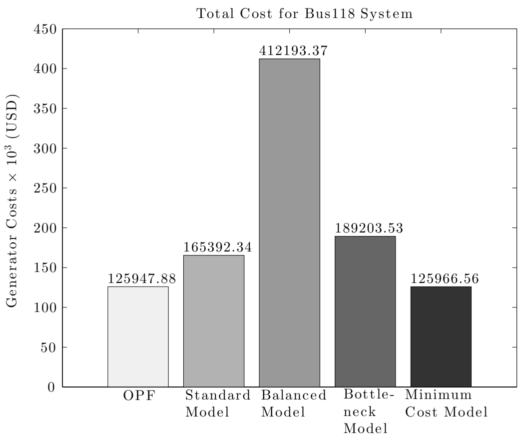

(d) Total power generation cost of all simple weighted flow models of this thesis.

Figure C.6.: Plots for the 118-bus electricity network.

Bibliography

[1] Distribution Loss Factor Calculation Methodology. *@ONLINE*, August 2004. URL `http://www.aer.gov.au/sites/default/files/Aurora%20-%20distribution%20loss%20factor%20calculation%20methodology.PDF`. Accessed: 2014-01-14. (Cited on page 15.)

[2] Ten-Year Network Development Plan 2012. *@ONLINE*, May 2012. URL `http://www.entsoe.eu/major-projects/ten-year-network-development-plan/tyndp-2012/`. Accessed: 2013-12-17. (Cited on page 34.)

[3] Swiss National Electricity Network. *@ONLINE*, February 2012. URL `http://www.geni.org/globalenergy/library/national_energy_grid/switzerland/swissnationalelectricitygrid.shtml`. Accessed: 2014-01-04. (Cited on page 11.)

[4] Winterkälte – Deutscher Strom rettet Frankreich. *@ONLINE*, February 2012. URL `http://www.manager-magazin.de/unternehmen/energie/a-814075.html`. Accessed: 2013-12-17. (Cited on page 34.)

[5] GUROBI OPTIMIZER – State of the Art Mathematical Programming Solver. *@ONLINE*, 2013. URL `http://www.gurobi.com/products/gurobi-optimizer/gurobi-overview`. Accessed: 2013-08-06. (Cited on page 8.)

[6] Resources – Power Systems Test Case Archive. *@ONLINE*, 2013. URL `http://www.ee.washington.edu/research/pstca/`. Accessed: 2013-08-13. (Cited on pages 2, 11, 12, 13, 27, 28, 29, 30, 32, 33, 35, 37, 38, 50, 54, 55, and 56.)

[7] MATLAB – The Language of Technical Computing. *@ONLINE*, 2013. URL `http://www.mathworks.com/products/matlab/`. Accessed: 2013-08-06. (Cited on page 8.)

[8] Electricity Monthly Update. *@ONLINE*, December 2013. URL `http://www.eia.gov/electricity/monthly/update/end_use.cfm#tabs_prices-3`. Accessed: 2014-01-14. (Cited on page 41.)

[9] Electricity Prices for Domestic Consumers. *@ONLINE*, December 2013. URL `http://appsso.eurostat.ec.europa.eu/nui/submitViewTableAction.do`. Accessed: 2013-12-27. (Cited on page 41.)

[10] Electricity Prices for Industrial Consumers. *@ONLINE*, December 2013. URL `http://appsso.eurostat.ec.europa.eu/nui/show.do?dataset=nrg_pc_205&lang=en`. Accessed: 2013-12-27. (Cited on page 41.)

[11] How we Balance the Country's Electricity Transmission System. *@ONLINE*, August 2013. URL `http://www.nationalgrid.com/uk/Electricity/AboutElectricity/Balancing+the+network/`. Accessed: 2013-08-14. (Cited on page 40.)

[12] Ultranet. *@ONLINE*, n/s. URL `http://www.amprion.net/netzausbau/ultranet-hintergrund`. Accessed: 2014-01-04. (Cited on page 52.)

[13] Steckbrief zum Projekt – Ultranet. *@ONLINE*, n/s. URL http://www.transnetbw.de/de/uebertragungsnetz/dialog-netzbau/osterath-philippsburg. Accessed: 2014-01-04. (Cited on page 52.)

[14] K. H. Abdul-Rahman and S. M. Shahidehpour. Application of Fuzzy Sets to Optimal Reactive Power Planning with Security Constraints. In *Power Industry Computer Application Conference, 1993. Conference Proceedings*, pages 124–130, 1993. doi: 10.1109/PICA.1993.291026. URL http://dx.doi.org/10.1109/PICA.1993.291026. (Cited on page 4.)

[15] M. A. Abido. Optimal Power Flow using Particle Swarm Optimization. *International Journal of Electrical Power & Energy Systems*, 24(7):563–571, 2002. ISSN 0142-0615. doi: 10.1016/S0142-0615(01)00067-9. URL http://dx.doi.org/10.1016/S0142-0615(01)00067-9. (Cited on page 5.)

[16] M. R. AlRashidi and M. E. El-Hawary. A Survey of Particle Swarm Optimization Applications in Electric Power Systems. *Evolutionary Computation, IEEE Transactions on*, 13(4):913–918, 2009. ISSN 1089-778X. doi: 10.1109/TEVC.2006.880326. URL http://dx.doi.org/10.1109/TEVC.2006.880326. (Cited on page 5.)

[17] S. Arora and B. Barak. *Computational Complexity: A Modern Approach.* Cambridge University Press, New York, NY, USA, 1st edition, 2009. ISBN 0521424267, 9780521424264. (Cited on page 7.)

[18] P. Attaviriyanupap, H. Kita, E. Tanaka, and J. Hasegawa. New Bidding Strategy Formulation for Day-Ahead Energy and Reserve Markets based on Evolutionary Programming. *International Journal of Electrical Power & Energy Systems*, 27(3):157–167, 2005. ISSN 0142-0615. doi: 10.1016/j.ijepes.2004.09.005. URL http://dx.doi.org/10.1016/j.ijepes.2004.09.005. (Cited on page 4.)

[19] M. Bläser and B. Manthey. Smoothed Complexity Theory. *CoRR*, abs/1202.1, 2012. doi: 10.1007/978-3-642-32589-2_20. URL http://link.springer.com/chapter/10.1007%2F978-3-642-32589-2_20. (Cited on page 7.)

[20] G. Bol. *Lineare Optimierung: Theorie und Anwendungen.* Athenäum Paperbacks. Athenäum-Verlag, 1980. ISBN 9783761050279. (Cited on pages 8 and 9.)

[21] B. Bollobas. *Graph theory: An Introductory Course.* Springer Verlag„ New York, 1979. Includes index. (Cited on page 7.)

[22] R. J. Brown and W. F. Tinney. Digital Solutions for Large Power Networks. *Power apparatus and systems, part iii. transactions of the american institute of electrical engineers*, 76(3):347–351, 1957. ISSN 0097-2460. doi: 10.1109/AIEEPAS.1957.4499563. URL http://dx.doi.org/10.1109/AIEEPAS.1957.4499563. (Cited on page 3.)

[23] L. J. Cai, I. Erlich, and G. Stamtsis. Optimal Choice and Allocation of FACTS Devices in Deregulated Electricity Market using Genetic Algorithms. In *Power Systems Conference and Exposition, 2004. IEEE PES*, volume 1, pages 201–207, 2004. doi: 10.1109/PSCE.2004.1397562. URL http://dx.doi.org/10.1109/PSCE.2004.1397562. (Cited on page 5.)

[24] J. Carpentier. Contribution to the Economic Dispatch Problem. *Bull. Sac. France Elect.*, 8(-):431–437, 1962. (Cited on page 3.)

[25] P.-H. Chen and H.-C. Chang. Large-Scale Economic Dispatch by Genetic Algorithm. *Power Systems, IEEE Transactions on*, 10(4):1919–1926, 1995. ISSN 0885-8950. doi: 10.1109/59.476058. URL http://dx.doi.org/10.1109/59.476058. (Cited on page 5.)

[26] T. S. Chung and Y. Z. Li. A Hybrid GA Approach for OPF with Consideration of FACTS Devices. *Power Engineering Review, IEEE*, 20(8):54–57, 2000. ISSN 0272-1724. doi: 10.1109/39.857456. URL `http://dx.doi.org/10.1109/39.857456`. (Cited on page 5.)

[27] G. B. Dantzig. *Maximization of a Linear Function of Variables Subject to Linear Inequalities, in Activity Analysis of Production and Allocation*, chapter XXI. Wiley, New York, 1951. URL `http://cowles.econ.yale.edu/P/cm/m13/m13-21.pdf`. (Cited on page 5.)

[28] Y. Del Valle, G. K. Venayagamoorthy, S. Mohagheghi, J.-C. Hernandez, and R. G. Harley. Particle Swarm Optimization: Basic Concepts, Variants and Applications in Power Systems. *Evolutionary Computation, IEEE Transactions on*, 12(2):171–195, 2008. ISSN 1089-778X. doi: 10.1109/TEVC.2007.896686. URL `http://dx.doi.org/10.1109/TEVC.2007.896686`. (Cited on page 5.)

[29] D. Devaraj and B. Yegnanarayana. Genetic-Algorithm-based Optimal Power Fow for Security Enhancement. *Generation, Transmission and Distribution, IEE Proceedings-*, 152(6):899–905, 2005. ISSN 1350-2360. doi: 10.1049/ip-gtd:20045234. URL `http://dx.doi.org/10.1049/ip-gtd:20045234`. (Cited on page 5.)

[30] J. A. Domínguez-Navarro, J. L. Bernal-Agustín, A. Díaz, D. Requena, and E. P. Vargas. Optimal Parameters of {FACTS} Devices in Electric Power Systems Applying Evolutionary Strategies. *International Journal of Electrical Power & Energy Systems*, 29(1):83–90, 2007. ISSN 0142-0615. doi: 10.1016/j.ijepes.2006.05.003. URL `http://dx.doi.org/10.1016/j.ijepes.2006.05.003`. (Cited on page 4.)

[31] L. A. Dunstan. Digital Load Flow Studies. *Power apparatus and systems, part iii. transactions of the american institute of electrical engineers*, 73(1):–, 1954. ISSN 0097-2460. doi: 10.1109/AIEEPAS.1954.4498891. URL `http://dx.doi.org/10.1109/AIEEPAS.1954.4498891`. (Cited on page 3.)

[32] J. Edmonds and R. M. Karp. Theoretical Improvements in Algorithmic Efficiency for Network Flow Problems. *J. ACM*, 19(2):248–264, Apr. 1972. ISSN 0004-5411. doi: 10.1145/321694.321699. URL `http://doi.acm.org/10.1145/321694.321699`. (Cited on page 6.)

[33] M. M. El-Saadawi, M. A. Tantawi, and E. Tawfik. A Fuzzy Optimization-based Approach to Large Scale Thermal Unit Commitment. *Electric Power Systems Research*, 72(3):245–252, 2004. ISSN 0378-7796. doi: 10.1016/j.epsr.2004.04.009. URL `http://dx.doi.org/10.1016/j.epsr.2004.04.009`. (Cited on page 4.)

[34] O. Elgerd. *Electric Energy Systems Theory: An Introduction.* Tata McGraw-Hill, 1983. ISBN 9780070992863. (Cited on page 14.)

[35] L. R. Ford and D. R. Fulkerson. Maximal Flow through a Network. *Canadian Journal of Mathematics*, 8:399–404, 1955. URL `http://www.rand.org/pubs/papers/P605/`. (Cited on page 6.)

[36] B. Gasbaoui and B. Allaoua. Ant Colony Optimization Applied on Combinatorial Problem for Optimal Power Flow Solution. *Leonardo Journal of Sciences*, 14:1–17, 2009. ISSN 1583-0233. URL `http://ljs.academicdirect.org/A14/001_017.pdf`. (Cited on page 5.)

[37] A. V. Goldberg and R. E. Tarjan. A New Approach to the Maximum Flow Problem. In *Proceedings of the Eighteenth Annual ACM Symposium on Theory of Computing*, STOC '86, pages 136–146, New York, NY, USA, 1986. ACM. ISBN 0-89791-193-8. doi: 10.1145/12130.12144. URL `http://doi.acm.org/10.1145/12130.12144`. (Cited on page 6.)

[38] A. V. Goldberg, E. Tardos, and R. E. Tarjan. *Flows, Paths and VLSI*, chapter Network Flow Algorithms, pages 101–164. In Korte et al. [49], 1990. ISBN 9783540526858. URL `http://www.springer.com/new+%26+forthcoming+titles+(default)/book/978-3-642-75766-2`. (Cited on page 6.)

[39] D. E. Goldberg. *Genetic Algorithms in Search, Optimization and Machine Learning*. Addison-Wesley Longman Publishing Co., Inc., Boston, MA, USA, 1st edition, 1989. ISBN 0201157675. (Cited on page 5.)

[40] W. Group. Common Format For Exchange of Solved Load Flow Data. *IEEE Transactions on Power Apparatus and Systems*, PAS-92(6):1916–1925, Nov. 1973. ISSN 0018-9510. doi: 10.1109/TPAS.1973.293571. URL `http://dx.doi.org/10.1109/TPAS.1973.293571`. (Cited on pages 11, 14, and 17.)

[41] H. Happoldt and D. Oeding. *Elektrische Kraftwerke und Netze*. Springer-Verlag GmbH, 1978. ISBN 9783540083057. URL `http://link.springer.com/book/10.1007%2F978-3-662-06962-2`. (Cited on pages 14, 20, 23, and 37.)

[42] J. M. Henderson. Automatic Digital Computer Solution of Load Flow Studies. *Power apparatus and systems, part iii. transactions of the american institute of electrical engineers*, 73(2):–, 1954. ISSN 0097-2460. doi: 10.1109/AIEEPAS.1954.4499023. URL `http://dx.doi.org/10.1109/AIEEPAS.1954.4499023`. (Cited on page 3.)

[43] J. Hindmarsh. *Electrical machines and their applications*. Pergamon international library of science, technology, engineering, and social studies. Pergamon Press, 1984. ISBN 9780080305721. (Cited on page 14.)

[44] N. Hingorani. Flexible AC transmission. *IEEE Spectrum*, 30(4):40–45, April 1993. ISSN 0018-9235. doi: 10.1109/6.206621. URL `http://dx.doi.org/10.1109/6.206621`. (Cited on page 1.)

[45] M. Huneault and F. D. Galiana. A Survey of the Optimal Power Flow Literature. *Power Systems, IEEE Transactions on*, 6(2):762–770, 1991. ISSN 0885-8950. doi: 10.1109/59.76723. URL `http://dx.doi.org/10.1109/59.76723`. (Cited on pages 1 and 3.)

[46] A. A. Ibrahim, A. Mohamed, and H. Shareef. Application of Quantum-inspired Binary Gravitational Search Algorithm for Optimal Power Quality Monitor Placement. In *Proceedings of the 11th WSEAS International Conference on Artificial Intelligence, Knowledge Engineering and Data Bases*, AIKED'12, pages 27–32, Stevens Point, Wisconsin, USA, 2012. World Scientific and Engineering Academy and Society (WSEAS). ISBN 978-1-61804-068-8. URL `http://dl.acm.org/citation.cfm?id=2183067.2183073`. (Cited on page 40.)

[47] T. Jayabarathi, K. Jayaprakash, D. N. Jeyakumar, and T. Raghunathan. Evolutionary Programming Techniques for Different Kinds of Economic Dispatch Problems. *Electric Power Systems Research*, 73(2):169–176, 2005. ISSN 0378-7796. doi: 10.1016/j.epsr.2004.08.001. URL `http://dx.doi.org/10.1016/j.epsr.2004.08.001`. (Cited on page 4.)

[48] R. Karp. Reducibility among combinatorial problems. In R. Miller and J. Thatcher, editors, *Complexity of Computer Computations*, pages 85–103. Plenum Press, 1972. URL `http://link.springer.com/chapter/10.1007%2F978-1-4684-2001-2_9`. (Cited on page 49.)

[49] B. Korte, L. Lovász, J. Pömel, and A. Schrijver, editors. *Flows, Paths and VLSI*. Algorithms and combinatorics. Springer-Verlag, Berlin, 1990. ISBN 9783540526858. URL `http://www.springer.com/new+%26+forthcoming+titles+(default)/book/978-3-642-75766-2`. (Cited on page 60.)

[50] V. Miranda and M. A. Matos. Distribution System Planning with Fuzzy Models and Techniques. In *Electricity Distribution, 1989. CIRED 1989. 10th International Conference on*, volume 6, pages 472–476, 1989. URL http://ieeexplore.ieee.org/xpl/articleDetails.jsp?arnumber=206126&navigation=1. (Cited on page 3.)

[51] V. Miranda and J. T. Saraiva. Fuzzy Modelling of Power System Optimal Load Flow. *Power Systems, IEEE Transactions on*, 7(2):843–849, 1992. ISSN 0885-8950. doi: 10.1109/59.141794. URL http://dx.doi.org/10.1109/59.141794. (Cited on page 3.)

[52] V. Miranda, M. A. Matos, and J. T. Saraiva. Fuzzy Load Flow – New Algorithms Incoorporating Uncertain Generation and Load Representation, 10th PSCC, Graz, August 1990. In *Proceedings of the 10th PSCC*. Butterworths, London, 1990. (Cited on page 3.)

[53] G. L. Nemhauser and L. A. Wolsey. *Integer and Combinatorial Optimization*. Wiley-Interscience series in discrete mathematics and optimization. Wiley, New York [u.a.], 1988. ISBN 0-471-82819-X. (Cited on page 8.)

[54] T. Niknam. A New Fuzzy Adaptive Hybrid Particle Swarm Optimization Algorithm for Non-Linear, Non-Smooth and Non-Convex Economic Dispatch Problem. *Applied Energy*, 87(1):327–339, 2010. ISSN 0306-2619. doi: 10.1016/j.apenergy.2009.05.016. URL http://dx.doi.org/10.1016/j.apenergy.2009.05.016. (Cited on page 4.)

[55] N/s. Final Report on the August 14, 2003 Blackout in the United States and Canada: Causes and Recommendations. Technical report, U.S.-Canada Power System Outage Task Force, 2004. URL http://www.ferc.gov/industries/electric/indus-act/reliability/blackout/ch1-3.pdf. (Cited on page 13.)

[56] T. P. O. of Science and Technology. Future Electricity Networks. pages 1–4, 2011. URL http://www.parliament.uk/documents/post/postpn_372-future-electricity-networks.pdf. (Cited on page 40.)

[57] J. Olivares-Galvan, P. Georgilakis, E. Campero-Littlewood, and R. Escarela-Perez. Core Lamination Selection for Distribution Transformers based on Sensitivity Analysis. *Electrical Engineering*, 95(1):33–42, 2013. ISSN 0948-7921. doi: 10.1007/s00202-012-0237-7. URL http://dx.doi.org/10.1007/s00202-012-0237-7. (Cited on page 14.)

[58] W. Ongsakul and P. Jirapong. Optimal Allocation of FACTS Devices to Enhance Total Transfer Capability using Evolutionary Programming. In *Circuits and Systems, 2005. ISCAS 2005. IEEE International Symposium on*, volume 5, pages 4175–4178, 2005. doi: 10.1109/ISCAS.2005.1465551. URL http://dx.doi.org/10.1109/ISCAS.2005.1465551. (Cited on page 4.)

[59] W. Ongsakul and T. Tantimaporn. Optimal Power Flow by Improved Evolutionary Programming. *Electric Power Components and Systems*, 34(1):79–95, 2006. doi: 10.1080/15325000691001458. URL http://dx.doi.org/10.1080/15325000691001458. (Cited on page 4.)

[60] T. J. Overbye, X. Cheng, and Y. Sun. A Comparison of the AC and DC Power Flow Models for LMP Calculations. In *37th Annual Hawaii International Conference on System Sciences, 2004. Proceedings of the*, page 9 pp. IEEE, 2004. ISBN 0-7695-2056-1. doi: 10.1109/HICSS.2004.1265164. URL http://dx.doi.org/10.1109/HICSS.2004.1265164. (Cited on pages 15 and 23.)

[61] N. P. Padhy. Congestion Management under Deregulated Fuzzy Environment. In *Electric Utility Deregulation, Restructuring and Power Technologies, 2004. (DRPT*

2004). Proceedings of the 2004 IEEE International Conference on, volume 1, pages 133–139, 2004. doi: 10.1109/DRPT.2004.1338481. URL http://dx.doi.org/10.1109/DRPT.2004.1338481. (Cited on page 4.)

[62] C. M. Papadimitriou. *Computational Complexity*. Addison-Wesley, Reading, Massachusetts, 1994. ISBN 0201530821. (Cited on page 7.)

[63] J. Peschon, D. S. Piercy, W. F. Tinney, O. J. Tveit, and M. Cuenod. Optimum Control of Reactive Power Flow. *Power Apparatus and Systems, IEEE Transactions on*, PAS-87(1):40–48, 1968. ISSN 0018-9510. doi: 10.1109/TPAS.1968.292254. URL http://dx.doi.org/10.1109/TPAS.1968.292254. (Cited on page 3.)

[64] V. C. Ramesh and X. Li. A Fuzzy Multiobjective Approach to Contingency Constrained OPF. *Power Systems, IEEE Transactions on*, 12(3):1348–1354, 1997. ISSN 0885-8950. doi: 10.1109/59.630480. URL http://dx.doi.org/10.1109/59.630480. (Cited on page 4.)

[65] S. S. Reddy, P. R. Bijwe, and A. R. Abhyankar. Faster Evolutionary Algorithm based Optimal Power Flow using Incremental Variables. *International Journal of Electrical Power & Energy Systems*, 54(0):198–210, 2014. ISSN 0142-0615. doi: 10.1016/j.ijepes.2013.07.019. URL http://dx.doi.org/10.1016/j.ijepes.2013.07.019. (Cited on page 5.)

[66] C. A. Roa-Sepulveda and B. J. Pavez-Lazo. A Solution to the Optimal Power Flow using Simulated Annealing. *International Journal of Electrical Power & Energy Systems*, 25(1):47–57, 2003. ISSN 0142-0615. doi: 10.1016/S0142-0615(02)00020-0. URL http://dx.doi.org/10.1016/S0142-0615(02)00020-0. (Cited on page 4.)

[67] A. Schrijver. On the History of the Transportation and Maximum Flow Problems. *Mathematical Programming*, 91(3):437–445, 2002. ISSN 0025-5610. doi: 10.1007/s101070100259. URL http://dx.doi.org/10.1007/s101070100259. (Cited on page 6.)

[68] H. Seifi and M. Sepasian. *Electric Power System Planning: Issues, Algorithms and Solutions*. Power Systems. Springer, 2011. ISBN 9783642179891. URL http://www.springer.com/engineering/energy+technology/book/978-3-642-17988-4. (Cited on page 16.)

[69] M. Shabani and M. R. A. Pahlavani. Fuzzy-based Multi-Objective Optimal Placement of Unified Power Flow Controller. *Applied Sciences Research*, 8(1):290–300, 2012. ISSN 1819-544X. URL http://www.aensiweb.com/jasr/jasr/2012/290-300.pdf. (Cited on page 4.)

[70] R. B. Shipley and M. Hochdorf. Exact Economic Dispatch – Digital Computer Solution. *Power apparatus and systems, part iii. transactions of the american institute of electrical engineers*, 75(3):–, 1956. ISSN 0097-2460. doi: 10.1109/AIEEPAS.1956.4499417. URL http://dx.doi.org/10.1109/AIEEPAS.1956.4499417. (Cited on page 3.)

[71] P. Somasundaram, K. Kuppusamy, and R. P. K. Devi. Evolutionary Programming based Security Constrained Optimal Power Flow. *Electric Power Systems Research*, 72(2):137–145, 2004. ISSN 0378-7796. doi: 10.1016/j.epsr.2004.02.006. URL http://dx.doi.org/10.1016/j.epsr.2004.02.006. (Cited on page 4.)

[72] Y. R. Sood. Evolutionary Programming based Optimal Power Flow and its Validation for Deregulated Power System Analysis. *International Journal of Electrical Power & Energy Systems*, 29(1):65–75, 2007. ISSN 0142-0615. doi: 10.1016/j.ijepes.2006.03.024. URL http://dx.doi.org/10.1016/j.ijepes.2006.03.024. (Cited on page 4.)

[73] E. Spring. *Elektrische Maschinen*. Springer-Lehrbuch. Springer, 2009. ISBN 9783642008856. URL http://books.google.de/books?id=ZH5f23QgHdMC. (Cited on page 14.)

[74] W. D. Stevenson. *Elements of Power System Analysis (McGraw-Hill electrical and electronic engineering series)*. McGraw-Hill, 3 edition, 1975. ISBN 0070612854. (Cited on page 14.)

[75] W. F. Tinney, V. Brandwajn, and S. M. Chan. Sparse Vector Methods. *Power Apparatus and Systems, IEEE Transactions on*, PAS-104(2):295–301, 1985. ISSN 0018-9510. doi: 10.1109/TPAS.1985.319043. URL http://dx.doi.org/10.1109/TPAS.1985.319043. (Cited on page 3.)

[76] M. Todorovski and D. Rajicic. An Initialization Procedure in Solving Optimal Power Flow by Genetic Algorithm. *Power Systems, IEEE Transactions on*, 21(2):480–487, 2006. ISSN 0885-8950. doi: 10.1109/TPWRS.2006.873120. URL http://dx.doi.org/10.1109/TPWRS.2006.873120. (Cited on page 5.)

[77] C. A. Trauth and R. E. Woolsey. Integer Linear Programming: A Study in Computational Efficiency. *Management Science*, 15(9):481–493, May 1969. ISSN 0025-1909. doi: 10.1287/mnsc.15.9.481. URL http://dx.doi.org/10.1287/mnsc.15.9.481. (Cited on page 10.)

[78] D. C. Walters. An Application of Genetic Algorithms to the Economic Dispatch of Power Generation. Master's thesis, Auburn University, May 1991. (Cited on page 5.)

[79] D. C. Walters and G. B. Sheble. Genetic Algorithm Solution of Economic Dispatch with Valve Point Loading. *Power Systems, IEEE Transactions on*, 8(3):1325–1332, 1993. ISSN 0885-8950. doi: 10.1109/59.260861. URL http://dx.doi.org/10.1109/59.260861. (Cited on page 5.)

[80] J. B. Ward and H. W. Hale. Digital Computer Solution of Power-Flow Problems. *Power apparatus and systems, part iii. transactions of the american institute of electrical engineers*, 75(3):–, 1956. ISSN 0097-2460. doi: 10.1109/AIEEPAS.1956.4499318. URL http://dx.doi.org/10.1109/AIEEPAS.1956.4499318. (Cited on page 3.)

[81] A. J. Wood and B. F. Wollenberg. *Power Generation, Operation, and Control*. John Wiley & Sons, New York, 1996. ISBN 9783761050279. URL http://www.scribd.com/doc/21295897/E-BOOK-Power-Generation-Operation-y-Control-Allen-Wood. Includes index. (Cited on pages vii, 16, 20, and 23.)

[82] I. K. Yu and Y. H. Song. A Novel Short-Term Generation Scheduling Technique of Thermal Units using Ant Colony Search Algorithms. *International Journal of Electrical Power & Energy Systems*, 23(6):471–479, 2001. ISSN 0142-0615. doi: 10.1016/S0142-0615(00)00065-X. URL http://dx.doi.org/10.1016/S0142-0615(00)00065-X. (Cited on page 5.)

[83] G. Zeitler. Vorstellung von TransnetBW am KIT. *@PRESENTATION*, 20.09.2013. (Cited on pages 18, 34, 43, 44, and 52.)

[84] R. D. Zimmerman and C. E. Murillo-Sanchez. User's Manual, 2011. URL http://www.pserc.cornell.edu/matpower/. (Cited on pages 2, 20, and 23.)

[85] R. D. Zimmerman, C. E. Murillo-sánchez, and U. A. D. Manizales. MATPOWER ' s Extensible Optimal Power Flow Architecture. Technical report, 2009. URL http://www.pserc.cornell.edu/matpower/. (Cited on pages 20 and 23.)

[86] R. D. Zimmerman, C. E. Murillo-Sanchez, and R. J. Thomas. MATPOWER's Extensible Optimal Power Fow Architecture. In *2009 IEEE Power & Energy Society General Meeting*, pages 1–7. IEEE, July 2009. ISBN 978-1-4244-4241-6. doi: 10.1109/PES.2009.5275967. URL `http://dx.doi.org/10.1109/PES.2009.5275967`. (Cited on pages 20 and 23.)

[87] R. D. Zimmerman, C. E. Murillo-Sanchez, and R. J. Thomas. MATPOWER: Steady-State Operations, Planning, and Analysis Tools for Power Systems Research and Education. *IEEE Transactions on Power Systems*, 26(1):12–19, Feb. 2011. ISSN 0885-8950. doi: 10.1109/TPWRS.2010.2051168. URL `http://dx.doi.org/10.1109/TPWRS.2010.2051168`. (Cited on pages 20 and 23.)